Abstract

SURFACTANT ASSISTED ELECTROSPRAY IONIZATION TIME OF FLIGHT MASS
SPECTROMETRY OF SYNTHETIC POLYMERS

by

James L. Brooks

July 2010

Chair: Dr. Ricky P. Hicks

Major Department: Chemistry

Synthetic polymers are complex mixtures which often require extensive characterization
to determine chemical composition and structure. Mass spectrometric techniques have greatly
enhanced the quantity, as well as the quality, of data that can be used to characterize synthetic
polymers. Electrospray Ionization Mass Spectrometry, ESI-MS, is capable of providing a wealth
of information on biomolecules, inorganic compounds, and small synthetic polymer (molecular
weight less than 3,000 g/mol). While ESI-MS has proven to be a powerful characterization
technique for small synthetic polymers its tendency to generate multiply charged ions results in
very complex data for higher molecular weight synthetic polymers and yields data that is too
complicated for complete analysis. A means to simplify the data obtained for ESI-MS
characterization of large synthetic polymers by reducing multiple charging and increasing signal
to noise ratio of the singly charged analyte ions would be of substantial use.

Singly charged poly (methyl methacrylate) ions with weight average molecular weights
4,000, 8,000 and 12,000 g/mol were observed by adding a surfactant (cetyltrimethylammonium
bromide) and changing critical ESI conditions. Altering these parameters, as well as others, has
played an important role of reducing the overall charging that the analyte may gain during the
desolvation process.

SURFACTANT ASSISTED ELECTROSPRAY IONIZATION TIME OF FLIGHT MASS

SPECTROMETRY OF SYNTHETIC POLYMERS

A Thesis

Presented To

the Faculty of the Department of Chemistry

East Carolina University

In Partial Fulfillment

of the Requirements for the Degree

Master of Science in Chemistry

by

James L. Brooks

July, 2010

SURFACTANT ASSISTED ELECTROSPRAY IONIZATION TIME OF FLIGHT MASS

SPECTROMETRY OF SYNTHETIC POLYMERS

by

James L. Brooks

APPROVED BY:

DIRECTOR OF THESIS: _____
                                                    Timothy J. Romack, PhD

COMMITTEE MEMBER: _____
                                                    Colin S. Burns, PhD

COMMITTEE MEMBER: _____
                                                    Paul W. Hager, PhD

COMMITTEE MEMBER: _____
                                                    Yumin Li, PhD

CHAIR OF THE DEPARTMENT OF CHEMISTRY:

_____
                                                    Ricky P. Hicks, PhD

DEAN OF THE GRADUATE SCHOOL:

_____
                                                    Paul J. Gemperline, PhD

ACKNOWLEDGEMENTS

I would like to thank my research advisor for helping me get through those tough semesters and guiding me from the beginning to the end of my research. Also, I would like to thank my committee members for being supportive throughout my project.

I would like to thank the Department of Chemistry for accepting me into their graduate program, providing me with the necessary tools to carry out my research, and financially supporting me.

Finally, to my family, thank you for teaching me that with hard work and determination I could get through anything.

TABLE OF CONTENTS

LIST OF TABLES

LIST OF FIGURES

LIST OF SCHEMES

LIST OF EQUATIONS

LIST OF ABBREVIATIONS

M_w	Weight Average Molecular Weight
M_n	Number Average Molecular Weight
PD	Polydispersity
GPC	Gel Permeation Chromatography
MALS	Multi Angel Laser Light Scattering
NMR	Nuclear Magnetic Resonance
MALDI	Matrix-Assisted Laser Desorption / Ionization
ESI	Electrospray Ionization
MS	Mass Spectrometry
m/z	Mass to Charge Ratio
DNA	Deoxyribonucleic Acid
EI	Electron Impact
CI	Chemical Ionization
ToF	Time of Flight
CRM	Charge Residue Mechanism
IEM	Ion Evaporation Mechanism
V	Voltage
C	Celsius
μL	Microliter
Q	Concentration of Excess Charge
i	Circuit Current
F	Faraday Constant

Γ	Flow Rate
x_c	Calculated PMMA Peak Mass to Charge Ratio Values
x_a	Actual PMMA Peak Mass to Charge Values

CHAPTER 1: BACKGROUND

"Polymers are composed of covalent structures many times greater in extent

than those occurring in simple compounds and this feature alone accounts

for the characteristic properties that set them apart from other forms of

matter. Appropriate means need to be used to elucidate their macromolecular

structure and relationships established to express the dependence of physical

and chemical properties on the structures so evaluated." – Paul Flory [1]

1.1 Brief History of Synthetic Polymers

Since the beginning of time polymers have existed as natural bio-molecules which are essential to life. The manufacture of synthetic polymers has been applied to a wide range of applications: cable insulation, car parts, packaging chips, kitchen appliances, paints, etc. The first published examples of synthetic polymers were vulcanized rubber and Bakelite. In the early 1800's natural rubber was an important commodity to the world but consequently it could only be used in limited environments because the natural rubber would become brittle if it became too cold or melt if it became too hot. In 1839 Charles Goodyear stumbled upon the synthesis of rubber that made it weather proof and the synthesis was given the title vulcanization [2]. In 1907 Leo Baekeland synthesized Bakelite, also known as polyoxybenzylmethylenglycolanhydride, which was important for its ability to act as an electrical insulator and its resistance to heat [3]. Up until the 1920's little was known about these large interconnected compounds (macromolecules) or if they were even interconnected, but Hermann Staudinger proved the existence of macromolecules with x-ray studies [4]. Staudinger was awarded the Nobel Prize in

Chemistry for his work in 1953. While Staudinger laid the debate of the interconnection of polymer chains to rest the behavior of polymers in solution was still an unfamiliar area. In 1953 Paul Flory proposed a temperature, theta temperature, at which the polymer chain obtains an ideal folded state. His theory helped to explain the behavior of both biological and synthetic polymers in solvents at their theta temperature and was awarded the Nobel Prize in Chemistry in 1974. Polymer science is considered to still be young and while it has taken large leaps and strides in the development and explanation of these complex systems, elucidation of large synthetic polymers with a quick and straightforward means still proves to be a challenge.

1.2 Introduction to Synthetic Polymers

Synthetic polymer samples are complex mixtures which often require extensive characterization to determine physical and chemical properties. They are complex due to the fact that a sample is composed of a distribution of molecular sizes, molecular structures, and shapes; to put it simply synthetic polymers are not

Figure 1: Possible Distribution of Molecular Sizes of a Polymer Sample

*mono*dispersed. **Figure 1** is an example of the distribution of macromolecules in a *poly*disperse
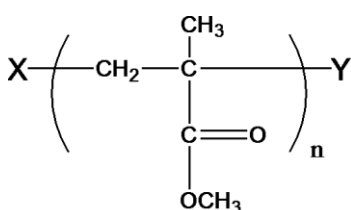
Figure 2: Poly (methyl methacrylate)

polymer. These polymers are made up of chemical units, also known as the backbone, that repeat sequentially depending on the synthesis. The characteristics of the repeat unit, as well as the bonding sequence, and identity of the end groups play an important role in the physical and chemical properties (**Figure 2**).

2

The n in Figure 2 represents the degree of polymerization, which corresponds to chain length of the polymer. Chain length of a polymer is important for its interactions with itself and with other compounds. In order to help describe these complex systems polymer chemist use weight average molar mass (M_w) (**Equation 1**), number average molar mass (M_n) (**Equation 2**), and polydispersity (PD) (**Equation 3**). The weight average molar mass takes into account the mass-average probability per molecule that a given macromolecule is present in the sample. The number average molar mass is the molecule number-average probability that a given macromolecule mass is present in the sample. Polydispersity is an index which utilizes both the weight average molar mass and number average molar mass help to describe how narrow or broad the polymer molecular mass distribution is.

Equation 1: Weight Average Molecular Weight

$$M_w = \Sigma_i N_i M_i^2 / \Sigma_i N_i M_i$$

Equation 2: Number Average Molecular Weight

$$M_n = \Sigma_i N_i M_i / \Sigma_i N_i$$

Equation 3: Poly Dispersity

$$PD = M_w / M_n$$

Where *N* in equations 1 and 2 represents the number of molecules, *M* is the molar mass of the ith molecules, and *i* is the selected molecule.

Synthetic polymers can be tailored to exist as hydrophobic, hydrophilic, high or low molecular weight, transparent, opaque, energy resilient, energy absorbing or any combination of these properties. All of these characteristics can be controlled by manipulating the chemical and

physical properties which are greatly influenced by molecular weight, molecular weight

distribution, chemical composition, chemical composition distribution, topology and end groups.

Due to the wide range of properties that polymers can have they make up a broad range

of many day to day applications that extends

Table 1: Synthetic Polymer Applications

Chemical Name	Application
Poly (methyl methacrylate)	Automotive Parts
Polytetrafluoroethylene	Teflon
Polyethylene	House Appliances
Polystyrene	Packaging Chips

from household goods to industrial tools.

Some of the synthetic polymers that have

proven to be of relevant importance include

Kevlar (poly paraphenylene terephthalamide) which is used in body armor, polyvinyl chloride's

which are commonly used for insulation and fluoropolymer's in lubricants. For more examples

of relevant synthetic polymers see Table 1. These synthetic polymers, as well as many more,

have made life much safer and more efficient. Challenging polymer samples can require

extensive characterization utilizing various analytical techniques to determine the aspects which

account for their distinct properties.

1.3 Typical Techniques of Analysis

As discussed earlier the broad range of properties of synthetic polymers can require

comprehensive characterization in order to identify the important physical and chemical

characteristics, which make their applications unique. It is important to reveal these key factors

governing the physical and chemical characteristics in order to understand the synthetic

polymer's functions. Insight into these characteristics can be explained by obtaining data on the

chemical composition, chemical composition distribution, molecular weight, molecular weight

distribution, topology, and end groups. Common techniques for the characterization of synthetic

polymers include gel permeation chromatography (GPC) / multi angle laser light scattering

4

(MALS), nuclear magnetic resonance (NMR), matrix-assisted laser desorption/ionization mass spectrometry (MALDI-MS), and electrospray ionization mass spectrometry (ESI-MS).

GPC separates polymer samples into several fractions which are then analyzed by one or more detectors (i.e. refractive index, ultraviolet detector, MALS). While GPC has proven to be a very important tool in yielding data on the weight average molecular weight, number average molecular weight and polydispersity of polymers, end group determination is not yet possible. End group determination of synthetic polymers is vital in that it contributes to the performance properties as well as reactivity.

NMR is capable of measuring the molecular weight and determining end groups of synthetic polymers, however determination of these two properties can only be elucidated under certain circumstances. As the length of the backbone increases (we can relate the overall length of the chain to the overall concentration of the sum of the backbone units) the concentration of the end group's decreases which directly affects the NMR signal strength.

MALDI-MS strength lies in its ability to singly charge large synthetic polymers creating simple and easy to interpret spectra. However, while MALDI-MS is considered to be a soft ionization technique it has been shown to fragment polymer end groups [5]. Soft ionization refers to a mass spectrometers ability to induce little, if any, fragmentation and minor loss non-covalent interaction. MALDI requires that the mixture of a matrix and analyte are soluble in a solvent so they can co-crystallize, however this can prove to be difficult with the available matrixes. Also, MALDI is not easily coupled to separation methods (i.e. high pressure liquid chromatography, capillary electrophoresis, and GPC) due to it being a pulsed ionization technique (produces packets of ions, not a continuous flow of ions).

ESI-MS has proven to be a very powerful technique in analyzing smaller synthetic polymers (i.e. molecular weight < 3,000 g/mol) yielding data on chemical composition, molecular weight, molecular weight distribution, and end groups [6, 7]. Multiple charging of analytes is considered to be a powerful feature for analyzing biomolecules, such as proteins and deoxyribonucleic acid (DNA), but this feature greatly limits the ability of ESI to characterize synthetic polymers. The multiple charging causes overlaying of peaks which make the spectra very complex and difficult to extract information from (**Figure 3**). Figure 3 shows the overlapping of one distribution of end groups that can be present on the synthetic polymer; however different end groups can cause variances in the molecular weight causing even further overlapping of peaks.
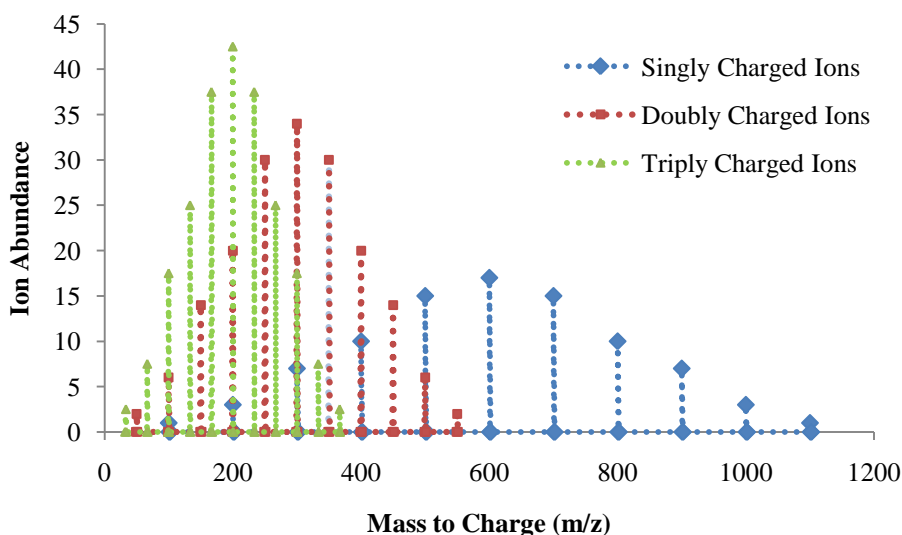
Figure 3: Example of ESI MS Multiple Charging of a Synthetic Polymer Sample

These, as well as other, characterization techniques have been coupled to one another in order to take advantage of all their strengths and to obtain a wide variety of data with just one run [8]. However, coupling of these instruments can be very time consuming and complex. So

6

while all of these characterization techniques have their strengths they have a core weakness that limits the amount of information which can be gathered from synthetic polymers. ESI-MS seems to be an appealing candidate for the analysis of larger molecular weight synthetic polymers if the charge state distribution could be controlled.

1.4 Overview of Mass Spectrometry

It is a common misconception that mass spectrometers measure the actual molecular weight of a compound, they actually measure the mass to charge ratio (m/z) versus the ion abundance. As a result of individual ions being measured the isotope effect must be accounted for and not an averaged mass. For example bromine has two naturally occurring isotopes ^{79}Br (natural abundance 50.7% and 78.92 g/mol) and ^{81}Br (natural abundance 49.3% and 80.92 g/mol) so two separate peaks will be detected at 78.92 and 80.92 m/z with the former peak consisting of a slightly higher ion abundance. A typical mass spectrometer consists of an ionization source, mass analyzer, and a detector (**Figure 4**).
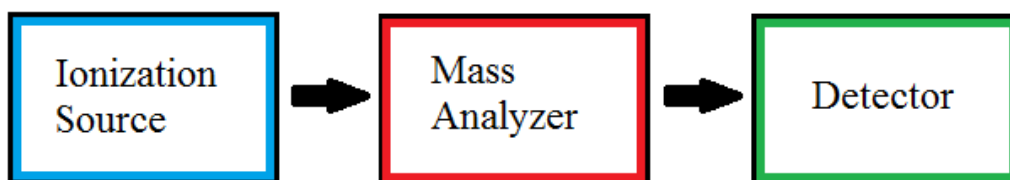
Figure 4: Components of a Typical Mass Spectrometer

1.4.1 Ionization Source

Perhaps the most vital process that occurs in a mass spectrometer is the formation of the ion. The ionization process is important because mass spectrometry requires gas phase ions to be created successfully. Fundamentally the sample must be ionized in order for the analyte to be separated and detected. There are many ionization techniques, some of particular importance are

electron impact (EI), chemical ionization (CI), matrix-assisted laser desorption/ionization (MALDI), and electrospray ionization (ESI). The first technique, EI, is considered to be a hard ionization technique (causes loss of covalent and non-covalent interaction) which is not optimal for acquiring reliable data on end groups and molecular weight distribution information. Also when using EI or CI the analyte must be volatile, thermally stable, and have a molecular weight less than 1,000 g/mol. MALDI and ESI are soft ionization techniques that permit the ionization of large nonvolatile compounds, like synthetic polymers.

1.4.2 Mass Analyzer

It is advantageous to be familiar with the molecular mass range of your analyte when selecting a mass analyzer because many mass analyzers have a set mass to charge range. Linear quadrupole and quadrupole ion traps mass to charge ranges do not exceed 6,000 m/z. This is not a crucial factor when working with low molecular weight compounds or when multiple charging higher molecular weight compounds that are *mono*disperse, but synthetic polymers can be very large well exceeding the mass of 6,000 g/mol. It is also important to note once again that synthetic polymers have a distribution of sizes and molecular weights associated with the sample, so the mass spectra will not have just one peak, it will have a distribution of peaks that vary over a large mass to charge range. The Time-of-Flight (ToF) mass analyzer has proven to be a very powerful ally when analyzing larger molecular weight compounds due the fact that the mass to charge range is theoretically unlimited.

Mass spectrometric techniques have significantly enhanced the quantity, as well as the quality, of data that can be obtained from many classes of compounds (i.e. catalyst, proteins, carbohydrates, etc.). Sensitivity, reproducibility, and automation have been established to be some of the features that make mass spectrometry so powerful. Mass spectrometry encompasses

a broad range of applications in fields such as inorganic chemistry, physical chemistry, biochemistry, medical chemistry, etc. However, the successful and complete elucidation of large synthetic polymers still proves to be an issue that has yet to be resolved.

1.5 Overview of ESI-MS

Electrospray was first investigated by Malcolm Dole over four decades ago [9], but was not brought to the analytical realm until 1984 by John Fenn [10]. Fenn was able to analyze low molecular weight analytes on an electrospray ionization quadrupole mass analyzer. In 2002 the Noble Prize in Chemistry was awarded to John Fenn and Koichi Tanaka for their work in the soft ionization techniques ESI and MALDI [11]. Their developments led to the analysis of higher molecular weight compounds that were both non-volatile and thermally labile.

While the process of ESI is straightforward it is important to understand how charge droplets are formed. A dilute sample (1-5 μM) is pushed through a capillary which has a high voltage (2 – 5 kV) applied to it. The high voltage causes a separation of positive and negative charges in solution. As the sample exits the capillary a Taylor cone is formed. Ions in solution eventually experience enough repulsive force to overcome the surface tension of the solvent and leave tip of the Taylor cone as a droplet. The droplets receive a push / pull to the mass analyzer from the applied electric field depending on the voltage implemented (**Figure 5**). Positive voltage at the capillary is typically applied for analyzing analytes that form positive ions, where as negative voltage at the capillary is typically applied for analyzing analytes that form negative ions [12].
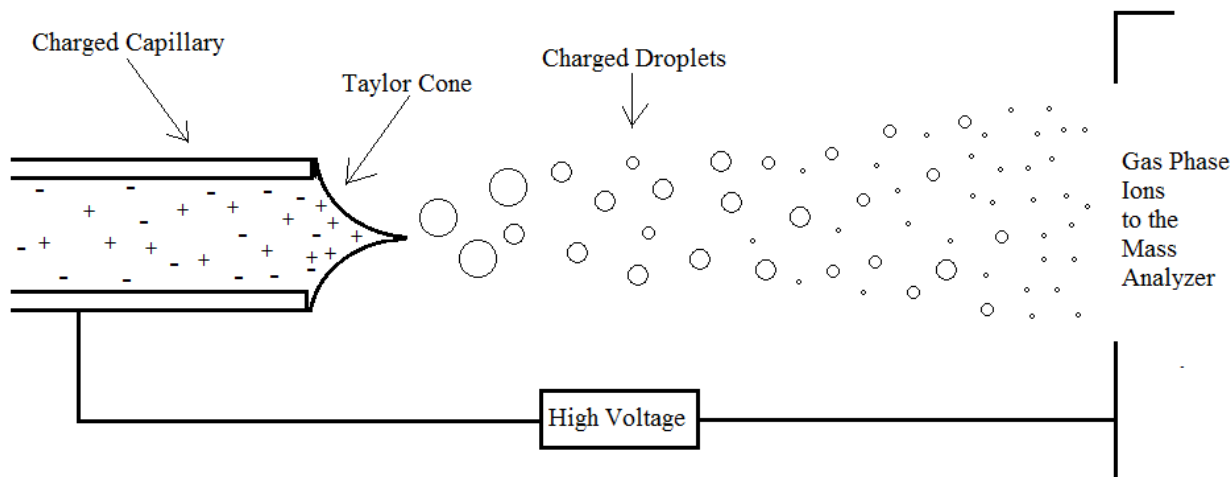
Figure 5: ESI Process

1.5.1 Production of Gas Phase Ions from Charged Droplets

There are two processes that have been proposed which explain how gas phase analyte ions form from charged droplets. After the droplet has ejected from the capillary it begins to travel towards the mass analyzer and the solvent starts to evaporate during which the charged residue mechanism (CRM) [9] or the ion evaporation model (IEM) [13] will be responsible for the production of gas phase ions. The mechanism by which the analyte is ejected into the gas phase is believed to be largely related to the analytes molecular size [14].

The charge residue mechanism is believed to be the mechanism of gas phase ion formation of larger compounds. As the droplet evaporates it eventually reaches a point where the
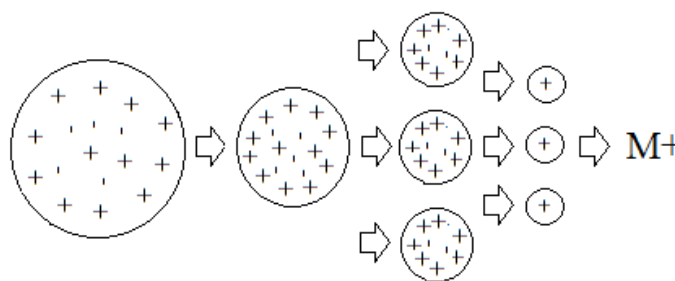
Figure 6: Charge Residue Mechanism

surface charge density is great enough for the droplet to undergo fission, this point is referred to as the Rayleigh limit [15]. The fission that takes place produces several offspring droplets from

the parent droplet, this process is repeated until one analyte molecule is present in one droplet, at this point the solvent evaporates and the analyte is released into the gas phase (**Figure 6**).

The ion evaporation model is believed to govern the gas phase ion formation for smaller compounds. During the IEM the droplet undergoes similar evaporation and fission events to that of
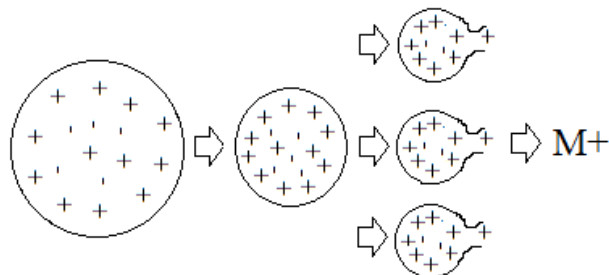
Figure 7: Ion Evaporation Mechanism

CRM; however at a critical diameter in the evaporation process coulombic repulsion forces the analyte to eject from the droplet surface to the gas phase in its ion form (**Figure 7**).

The CRM and IEM are different in the way by which the analyte in the droplet is released to the gas phase as ions. We are more interested in the charge residue mechanism (CRM) because the synthetic polymers that we wish to analyze are considered to be large compounds.

1.6 What We Know About ESI-MS

Solvent selection plays an important role in the observed analyte charge state. Multiple charging of the analyte in the positive ion mode results from the attachment of several protons or several cations. Use of higher polarity solvents has been shown to favor the formation of higher charge states because it improves stability of charge separation in solution [16]. Improved stability of charge separation in solution can hinder the ability of the counterion to move to the parent and offspring droplets during the droplet fission process. This decreases the overall ion pairing during the solvent evaporation and droplet fission process.

The range of solvents in ESI is limited to those with higher dielectric constants (20 - 80). This is due to the fact that ESI solvents must be capable of conducting charge. Typically with an

increase in the dielectric constant of the solvent the surface tension also increases. It has been

seen that if the surface tension of the solvent is increased the charge state of the analyte will also

be increased [17]. The surface tension increases the time it takes the droplet to reach the

Rayleigh limit which effectively enhances the amount of charges that can exist on the surface of

the droplet before fission occurs. This will result in higher concentration of charges in the

offspring droplet. The rise in the number of charges that will exist in the droplet surface

increases the likely hood for the analyte to obtain more than one charge as it enters the gas phase.

It is also important to note the solubility of analytes in the solvent, i.e. better solvated ions have

lower partitioning constants and hence will have a lower ESI response [18].

Analytes with the highest response have been shown to have both a polar and a nonpolar

character. The polar portion can help to facilitate charging while the nonpolar character of an

analyte causes it to exist on the surface of the droplet. This is because the solvents typically

employed are polar so the partitioning constant of the nonpolar character will be higher than that

of a analyte with a large polar character [19]. Also the atmospheric environment of the droplet is

considered to be nonpolar, so the analyte will partition to the nonpolar phase. Analytes that

exhibit a higher degree of surface activity will have higher intensity signals because these surface

active analytes exhibit greater desorption characteristics [20] (**Figure 8**). Figure 8 shows how a

surface active compound (A) has a much greater probability of being in the offspring droplet

during the fission process then a compound that exists in the core of the droplet (B).
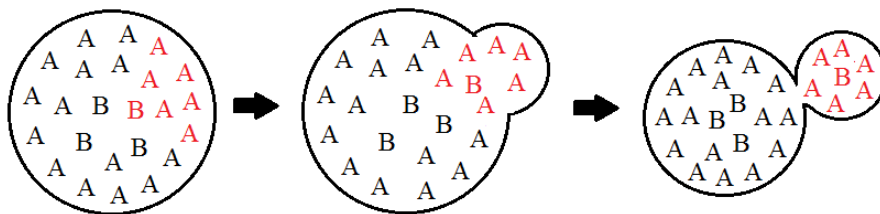
Figure 8: Surface Active Analytes have a Higher ESI Response

1.7 Surfactants

Surfactants are surface active compounds that contain a polar (hydrophilic) head and a nonpolar (hydrophobic) tail, this property of a compound is also typically identified as being amphiphlic (**Figure 9**). Surfactants have a broad range of usages and can be found in various products such as detergents, shampoos, paints, and dental floss. They are soluble in nonpolar and polar environments, which allow it to act as a phase interface transferring agent. However to our knowledge the unique and diverse range of properties that are derived from there amphiphlic character has not been applied to ESI-MS of synthetic polymers. Based on the literature it is believed that certain surfactants will have a very high ESI response even at a low concentration due to the nonpolar character and its ability to have a stable charge. If a surfactant is able to associate with an analyte acting as the charging agent then it may be brought to the surface of the droplet.

Nonpolar Tail   Polar Head
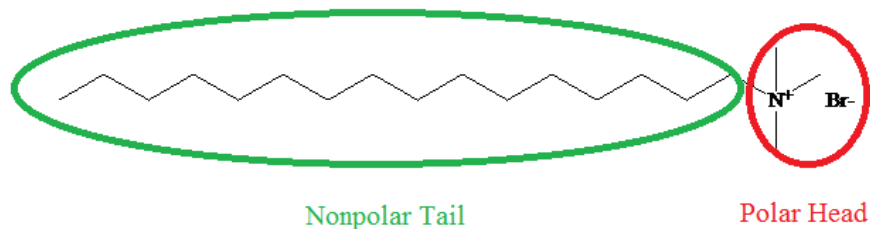
Figure 9: Cetyltrimethylammonium Bromide

1.8 ESI-MS of Synthetic Polymers

ESI-MS is considered to be a very soft ionization technique that limits the amount of fragmentation and decomposition of synthetic polymers. The limited amount of decomposition and fragmentation that takes place allows for the reliable determination of end groups and molecular weight distribution data. While this feature of ESI is advantageous for lower molecular weight polymers, larger molecular weight polymers are still plagued by the multiple charging that occurs which creates spectral congestion due to peak overlap.

As stated earlier ESI has a limited solvent selection, depending on the analyte being analyzed, due to conductivity requirements. Typical ESI solvents include, but are not limited to, methanol, acetonitrile, and water. Various solvents can be mixed and matched to meet suitable conductivity requirements, but solubility of the analyte can still be an obstacle here. Most industrial and household synthetic polymers are nonpolar and require such solvents to be dissolved in. Researchers have utilized additives that act as conductivity enhancers to attempt to deal with this polymer solubility and solvent conductivity issue [21]. However, the lower m/z region is congested by the conductivity enhancer and this does not deal with the issue of complex spectra that are created by multiple charging.

A powerful feature of ESI is the ability to carefully modify the amount of energy that can be imparted to the analyte. The potential that is applied to the capillary is one of the essential parameters to obtaining a sustainable Taylor cone. It was seen that high cone voltage produced higher intensity spectra of the lower molecular weight singly charged synthetic polymer ions [22]. Larger gas phase ions of lower charge states do not experience the same amount of focusing towards the skimmer. The increased energy imparted to the analyte also promotes

14

charge shedding. Charge shedding is the transfer of charge from the analyte to neutral gas

molecules or species that were present in the sample and solvent.

To our knowledge ESI-ToF-MS has not been utilized to successfully analyze poly(methyl

methacrylate) samples above the mass range of 4,000 g/mol without an offline/online separation

technique or data processing assistance [23].

CHAPTER 2: ELECTROSPRAY IONIZATION OF POLY (METHYL METHACRYLATE)

The previous chapter attempts to give insight into synthetic polymers and to introduce electrospray ionization time of flight mass spectrometry as a possible aid in elucidation of these large complex mixtures. The objective of this thesis is to develop a means to obtain ESI-MS spectra of poly (methyl methacrylate) that contains almost exclusively singly charged peaks. We believe that clean and easy to interpret ESI spectra can be obtained by adding a compound that is surface active, associates with the polymer and is easily ionizable. A large bulky surface active compound, like a surfactant, should associate with the polymer and bring it to the gas phase before additional charge attachment can occur. This research should extend the reach of ESI-MS to much larger synthetic polymers that have been otherwise unobtainable due to complex spectra.

2.1 Results and Discussion

2.1.1 Critical Parameters

One of the powerful tools of ESI is the ability to fine tune several of the ionization parameters. It is important to adjust electrospray parameters to favor the formation of a droplet that contains one macromolecule and one charging agent. Once this offspring droplet completely evaporates a singly charged macromolecule will be present and analyzed. The following parameters were chosen based upon that goal (**Table 2**):

Table 2: ESI Parameters

Parameter	Setting
Capillary Voltage	2900
Sample Cone Voltage	100-150
Extraction Cone Voltage	2.0
Source Temperature (°C)	90
Desolvation Temperature (°C)	150
Cone Gas Flow Rate (L/hr)	0

Desolvation Gas Flow Rate (L/hr)	500
Syringe Pump Flow Rate (µL/min)	5.0-10.0

These parameters have been tested to yield the maximum amount of singly charged

analyte ions of PMMA in acetone with surfactant, while being conscious of possible

fragmentation. Figure 10 helps the reader to visualize the location of each parameters source in

the ionization process.
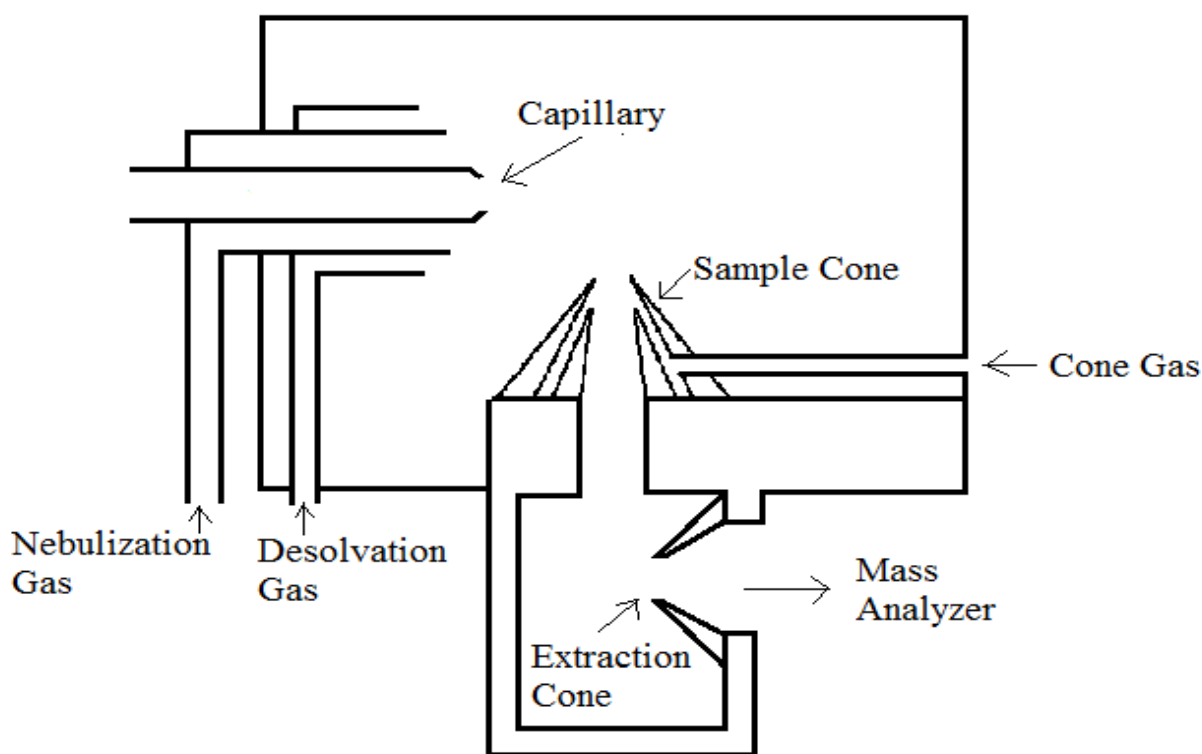
Figure 10: Internal Scheme of Electrospray Ionization [28]

Capillary voltage is usually set at about 3000 V for most samples; however it is

important to tune this in order to achieve a stable Taylor Cone. Based on experiments that were

conducted it was seen that an increase in the capillary voltage resulted in an increase in the total

ion count but no apparent decrease in the doubly charged peaks. Lowering the overall capillary

voltage lowered the overall ion intensity, but no change in multiple charging was clearly present

as its ion intensity decreased along with the singly charged ion intensity. Increasing the capillary voltage to a high setting can possibly cause fragmentation of the macromolecule so a capillary voltage of 2900 was chosen.

The *sample cone voltage* is typically adjusted for the type of analyte being analyzed, i.e. solvent, carbohydrates, protein ions, etc. Higher molecular weight analytes can require higher sample cone voltage to observe appropriate distributions. Based on the ESI q-ToF manual the sample cone voltage should be adjusted for maximum sensitivity, within the range 15V to 150V. When increasing the sample cone voltage it is important be aware of possible analyte fragmentation. Increasing the voltage leads to higher analyte kinetic energy which results in a higher probability of collisions [24]. The sample cone voltage was adjusted for each sample to achieve the maximum amount of singly charged ions.

Extractor cone voltage is typically optimizes within the range of 0 - 5V. Adjusting the voltage to higher values may cause fragmentation of analyte ions. An extractor cone voltage of 2.0 appears to be appropriate for the poly (methyl methacrylate) standards.

Cone gas flow rate is typically altered to reduce the possible adduct ions or solvent clustering ions. If the cone gas flow rate is set to 0 then it is possible to increase the length of time that a low surface-charge density is present before droplet fission occurs, hence leading to offspring droplets with less overall charge.

The *desolvation gas* is heated and distributed as a coaxial sheath to the analyte as it is sprayed. Based upon our experiments increasing the desolvation gas temperature to 200° C appeared to decrease the amount of doubly charged ions and decreasing the desolvation temperature to 100° C appeared to increase the doubly charged ions. This is not consistent with

research that states that rapid evaporation of charged droplet should lead to higher charged states [25]. However it is possible that the temperature is affecting the overall solubility of the polymer, causing it to develop a closed or compact form. Also the increase of the viscosity of the droplet would hinder the ability of the analyte to move to the surface and gain charge [26]. The desolvation gas temperature was set to 150° C in order to diminish the amount of multiple charging while keeping the amount of energy introduced to the system low enough to prevent possible fragmentation.

In our studies of varying the *gas desolvation flow rate* it did not appear to alter the doubly charged region or the ion intensity in any great effect. However, increasing the gas flow rate to values higher than the amount quoted in the q-ToF manual leads to high nitrogen levels. High levels of nitrogen could possibly cause an enhanced amount of collisions between the gas molecules and analyte ions, but this is not likely. However, possible amplified amount of collisions could cause charge shedding but could also induce fragmentation of labile groups.

The *syringe pump flow rate* is directly related to the amount sample consumed however does not alter the amount of energy in the system. Increasing the syringe pump flow rate from 5.0 uL/min to 15.0 uL/min reduced the multiply charged region, as well as increased the overall ion intensity. Based upon the literature using higher flow rates will create droplets with a lower density of charge per unit volume [27].This can be explained by the excess charge equation listed below:

Equation 4: Concentration of Excess Charge

$[Q] = i / F\Gamma$

Where [Q] represents the concentration of excess charge, i is the circuit current (amperes), F is Faraday's constant (96,485 coulomb/mol), and Γ is the flow rate (L/sec). Offspring droplets that separate from the parent droplets when the surface charge density is low will contain fewer charges [16]. The sample flow rate was adjusted for each sample as to optimize the amount of sample consumed, the time it takes for successful analysis, and to reduce the amount of multiple charging. For sample consumption purposes the syringe pump flow rate above 10.0 uL/min will not be used as it produced a respectable ion intensity value as well as decreases the multiple charging.

2.1.2 Solvent Selection

Selecting a solvent plays a considerable role in the conformation which a polymer assumes in solution. We want a solvated polymer so isolated chains in solution form and the polymer does not attach to one another forming large coalesced balls. A solvent that is not highly polar and our analyte is soluble in would be suitable for ESI analysis. Acetone seems like an appropriate candidate for our study with a low dielectric constant, compared to typical ESI solvents (acetone at 21, methanol at 33, acetonitrile at 36, and water at 80), as well as a low surface tension.

2.2 ESI-MS of Poly (Methyl Methacrylate)

Based upon the literature high molecular weight poly (methyl methacrylate) standards have not yielded ESI-MS spectra dominated by singly charged ions. Poly (methyl methacrylate), PMMA, has an extensive array of properties that can depend on its molecular weight, molecular weight distribution, and end groups. PMMA can have good resistance to effects of weathering while being a transparent tough material. This synthetic polymer has found applications in lenses, skylight domes, protective coatings, and riot shields [29].

2.2.1 Analysis of PMMA 4000

We began our research of the PMMA series by trying to create a spectra just utilizing PMMA 4000 without the addition of any chemical additives and under optimized parameters (**Figure 11**).
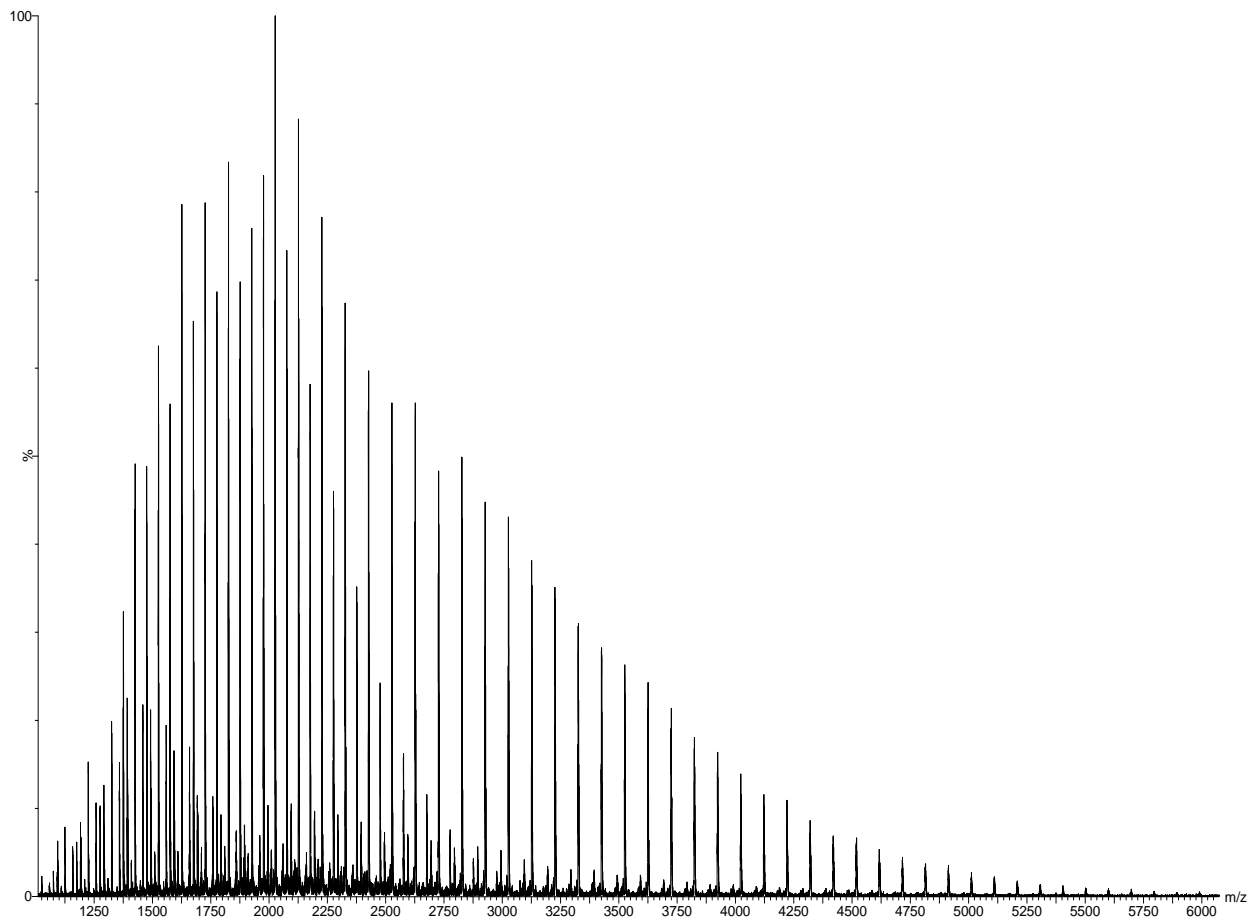
Figure 11: ESI-ToF of PMMA 4000 without a cationizing agent at optimized parameters

We found that even if we ran PMMA 4000 under the optimized conditions that would promote the greatest amount of singly charged gas phase ions a large amount of the multiple charging was still present. Singly charged ions can be found by measuring the m/z difference between an adjacent peak. If the difference is 1 then it is singly charged or if it is 0.5 then it is

21

doubly charged. The large amount of multiple charging that takes place contributes to the overall ion intensity of the singly charged peaks, $[M + Cation]^+$, due to peak m/z overlapping. Calculating the number average molecular weight, weight average molecular weight and polydispersity will be perturbed by the overlapping ion intensity contribution. Also the congestion in the lower ion intensity region requires additional deconvoluting to draw information from. The lower intensity regions of these spectra can give insight into different end groups of the polymer, possible contaminates present in the sample and/or other charging agents present.

By adding our surfactant, cetyltrimethylammonium bromide, to the sample prior to injection into the ESI-ToF, along with the optimized settings, we are able to create a spectrum that is dominated by singly charged peaks, $[M + CTA]^+$ that dwarfs the now lower ion intensity doubly charged region (**Figure 12**).
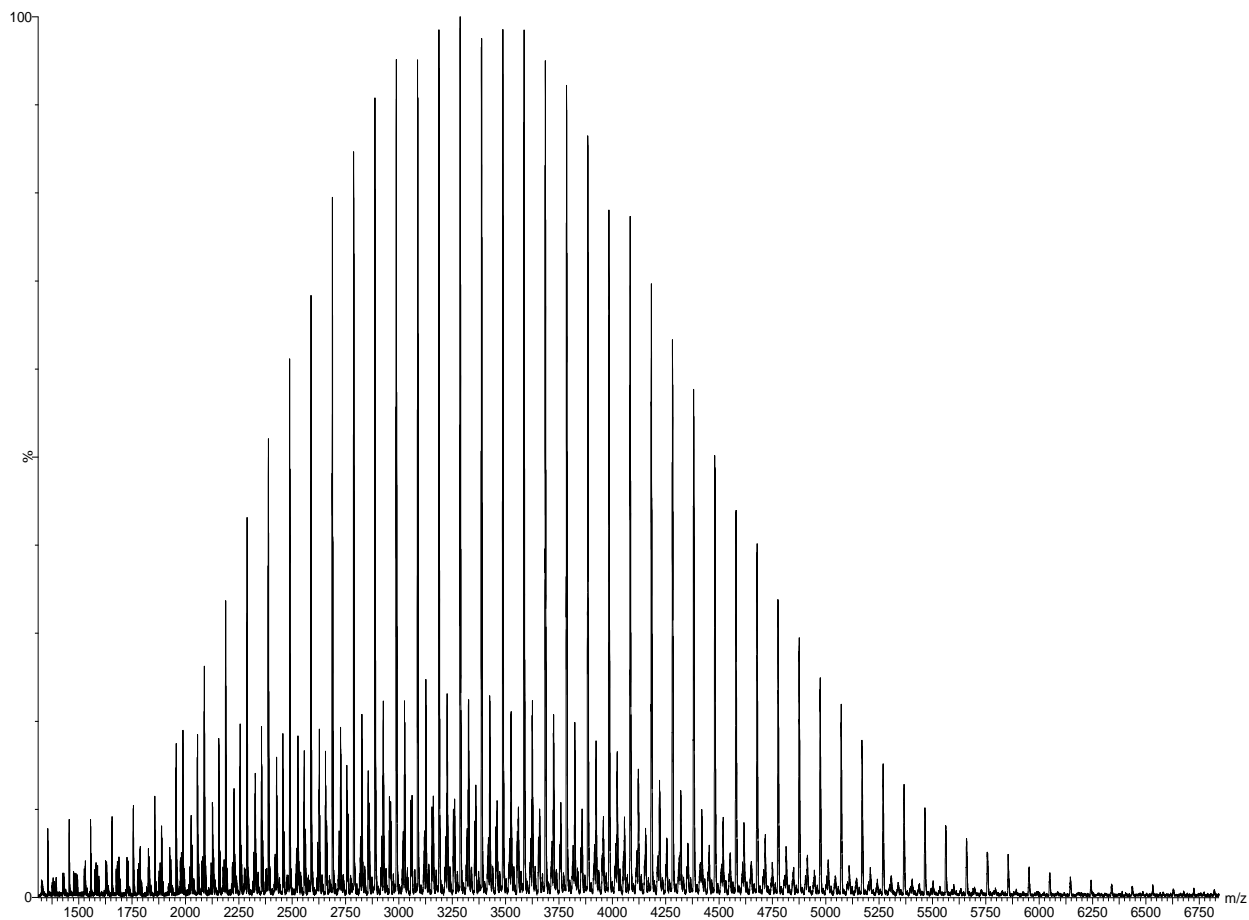
Figure 12: ESI-ToF of PMMA 4000 with the addition of cetyltrimethylammonium bromide under optimized conditions

The clean distribution of peaks from Figure 12 allows the simple calculation of the

number average molecular weight, weight average molecular weight, and polydispersity

(**Equations 1, 2, and 3**). A calibration correction had to be applied because the ESI-ToF was

only calibrated in the lower molecular weight range (100 – 2000 m/z) in which the polymer mass

distribution far exceeds (> 6000 m/z). A calibration line and equation was generated in excel by

plotting exact peak m/z calculations of PMMA (with hydrogen end groups) and a

cetyltrimethylammonium ion masses from the isotope calculator on MassLynx. A second

calibration line and equation was generated with actual uncorrected peak data from the ESI-ToF

spectrum of PMMA 4000. A sixth order polynomial fit was the best fit for the uncorrected peak

23

data. The y- axis is set as the backbone repeat unit associated with each macromolecule. Each

equation generated is set equal to one another and then x_c is solved for.
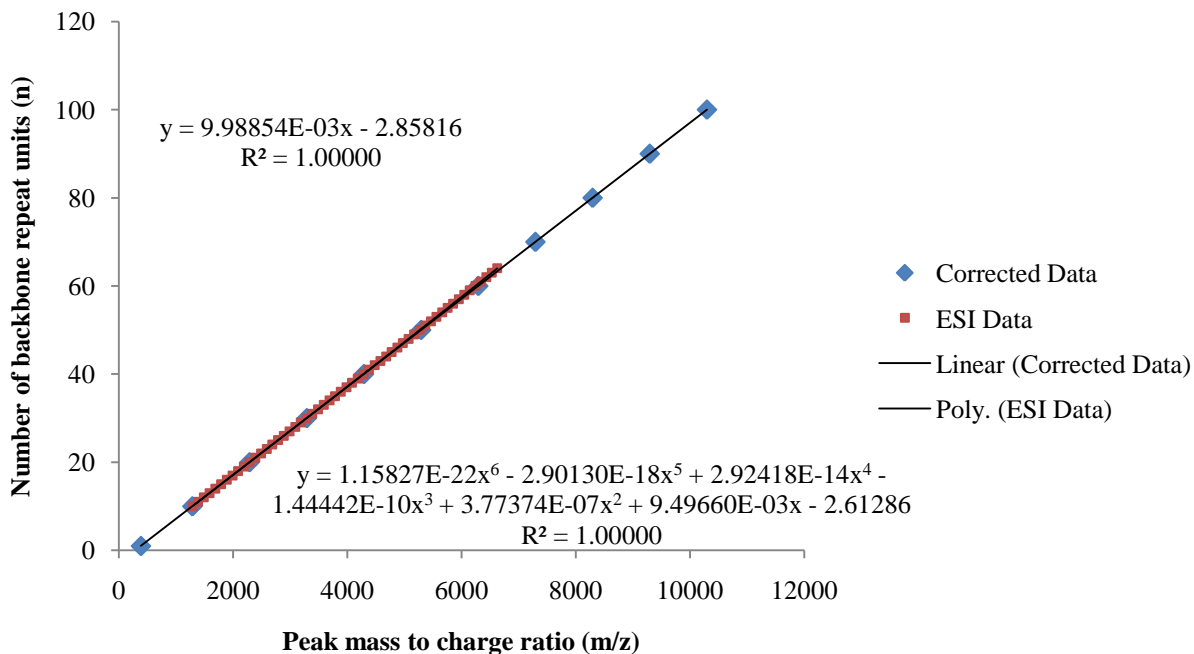
Figure 13: Calibration lines generated from corrected and actual ESI data points

The actual m/z, intensity, and corrected m/z of each peak can be found in Table 3. When

contacting Waters concerning our dilemma of coming across a method and/or sample that could

help us calibrate the instrument for such a broad mass to charge range (100 – 7000 m/z) they

were surprised by our request and could only give little insight into solving the problem. This is

perhaps due to the fact that not many larger molecular weight polymers have been analyzed on

an ESI-ToF instrument because of the multiple charging and congested spectra that would be

created.

Table 3: The actual m/z, intensity, and corrected m/z of PMMA 4000

Actual m/z	Intensity	Corrected m/z			
1387.0931	8	1386.8645	4083.6096	369	4090.3602

24

1487.1329	12	1486.7767	4182.7554	297	4190.3850
1588.1923	15	1587.7766	4281.8633	270	4290.4564
1688.2686	20	1687.8478	4380.8257	246	4390.4693
1788.3169	25	1787.9320	4479.7881	214	4490.5740
1888.3674	35	1888.0494	4579.5825	187	4591.6168
1988.3804	81	1988.1525	4678.3066	171	4691.6744
2088.4080	112	2088.2873	4775.9565	144	4790.7425
2188.4202	143	2188.4198	4875.5557	126	4891.8927
2288.4287	184	2288.5588	4974.0425	106	4992.0197
2388.3948	222	2388.6646	5072.1992	93	5091.9191
2488.3406	260	2488.7591	5169.6133	76	5191.1719
2588.2805	291	2588.8579	5268.5703	65	5292.1109
2688.1929	339	2688.9414	5366.6226	55	5392.2435
2788.0654	361	2789.0000	5464.6636	43	5492.4834
2887.8955	387	2889.0347	5561.9966	35	5592.1206
2987.4190	405	2988.7845	5659.5723	28	5692.1310
3087.5149	405	3089.1352	5756.2295	22	5791.3274
3187.2622	420	3189.1683	5854.2622	21	5892.0698
3286.9307	426	3289.1591	5952.5537	15	5993.2199
3387.6172	415	3390.2139	6049.7388	12	6093.3773
3487.1968	420	3490.2052	6145.5884	10	6192.3075
3586.7632	419	3590.2358	6243.1260	8	6293.1406
3686.2539	405	3690.2479	6339.5972	6	6393.0401
3785.6951	393	3790.2730	6437.2598	5	6494.3553
3885.0593	368	3890.2882	6532.5767	6	6593.4258
3984.3513	332	3990.3028	6628.0586	4	6692.8683

It is important to validate our molecular weight calculations from the ESI spectrum, so an In-lab GPC on our PMMA 4000 standard was run and compared the values obtained (**Table 4**).

Table 4: Molecular weight distribution data from ESI-ToF calculations, In-Lab GPC, and Manufacturer GPC of PMMA 4000

Technique	Mw	Mn	PD
ESI - ToF	3480	3256	1.07
In-Lab GPC	3728	3497	1.07
Manufacturer GPC	4200	3900	1.06

A percent difference equation was used to test the precision of or calculated molecular weight data (**Equation 5**).

Equation 5: Percent Difference

Percent Difference $= |(x_1 - x_2) / ((x_1 + x_2)/2)| \cdot 100$

The In-lab GPC values reveals that our weight average molecular weight percent difference from the ESI calculations is only 6.6%. Whereas the percent difference of weight average molecular weight of the In-lab GPC values and ESI-ToF values from the manufacturer GPC values are respectively 11.9% and 18.9%. The In-lab GPC's calibration line was created with polystyrene standards, so a variation in molecular weight calculation is possible when analyzing other polymers. Based on our results the ESI-ToF calculations appear to have a good correlation with our In-Lab GPC calculations.

Another important piece of data that can be determined is the number of backbone repeat units and end groups of each peak. The major distribution shown in Table 3 is determined to have two hydrogen's as the end groups. The manufacturer was contacted and confirmed hydrogen's as the end groups. The calculation shown below is an example of how to determine the end groups from peak mass to charge ratio.

The molecular weight of the cationizing agent is first subtracted from the observed mass.

4290.4594 m/z – 284.3317 m/z = 4006.1247 m/z

Next the mass of the sum of the number of backbone units is subtracted.

Approximate number of backbone repeat units (n) = 40

$$4006.1247 \text{ m/z} - 4004.1040 \text{ m/z} = 2.0207 \text{ m/z}$$

2.0207 is approximately the mass of two hydrogen atoms (2.0157 g/mol)

Table 5 below summarizes the major species present in the ESI spectrum of PMMA 4000.

Table 5: Assigned Possible Structures to Peaks of PMMA 4000

	Assigned Structure	m/z assignments	
		$[M+CTA]^+$	$[M+Na]^+$
A		4290.4564	3127.9604
B		3363.1094	N/A
C		2256.4813	1995.1981

In Table 5 there are three distinct structures A, B, and C. Structure A is the dominant species present and the expected major product in the sample. Structure B is assigned a structure

27

which would have residual trimethylsilyl still present in the sample. While structure C is

believed to be an oligomer that has been fragmented. This fragmentation was not expected

because of ES soft ionization ability. During growth transfer polymerization (GTP) there is an

initiation, propagation, and termination step [30]. An initiator is employed to attach the

trimethylsilyl group to a monomer unit and facilitates the group transfer to another monomer unit

initiating a carbon-carbon bond through Mukaiyama-Micheal reactions (**Scheme 1**) [31, 32].

Scheme 1: Group Transfer Polymerization Mechanism
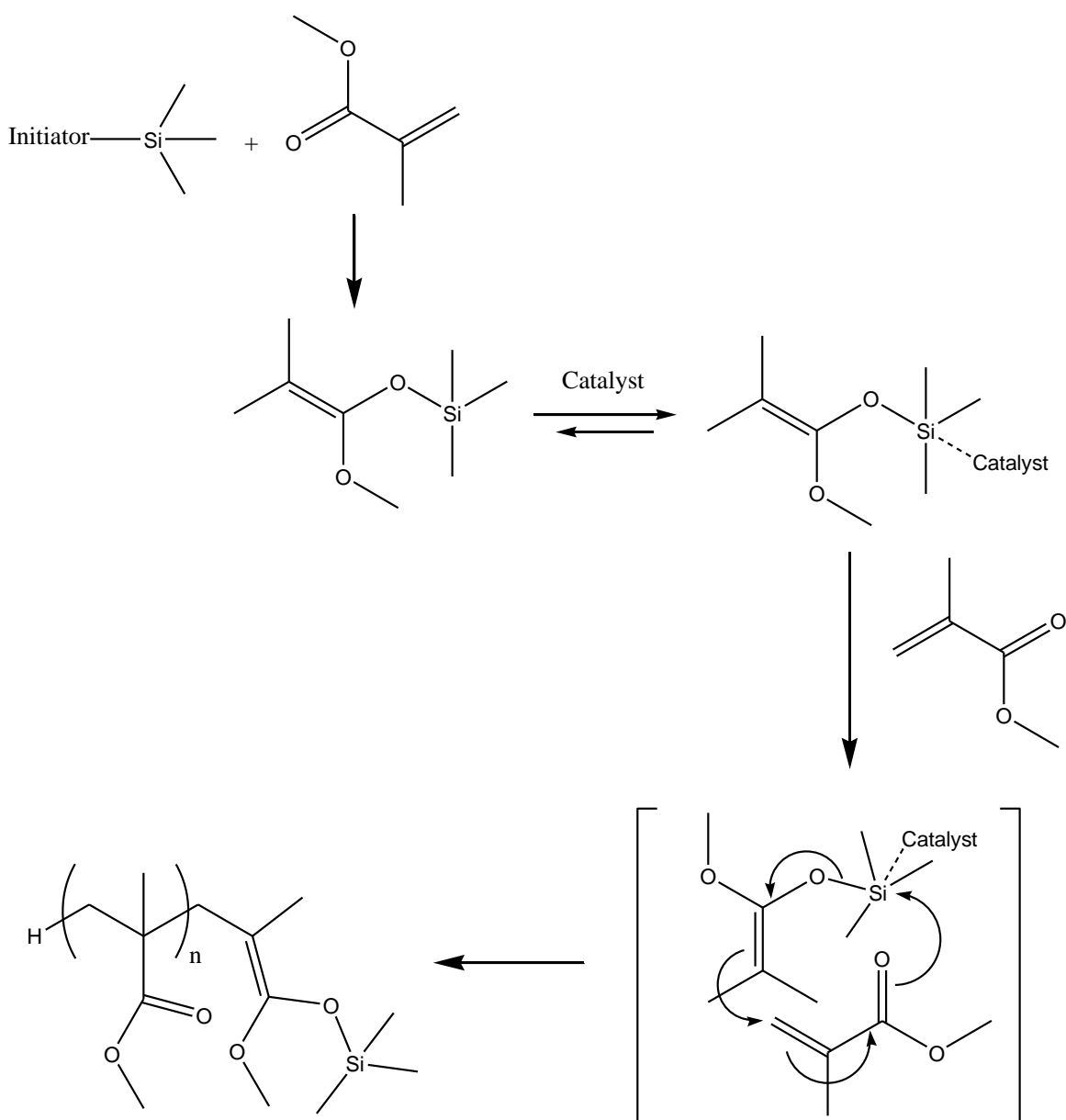
It is possible that not all of the trimethylsilyl was terminated and could still be present on the end of the oligomer. The carbon-oxygen bond (*), assigned to structure B, is more labile due to the diminished electron withdrawing nature of the oxygen by the trimethylsilyl group. This increases the ability to stabilize the carbocation after the bond scission. It is reasonable to believe

that the fragmentation is occurring at this labile bond rather than the ester bond present in assigned structure A.

In order to further confirm that there is trimethylsilyl present in the sample we ran a proton NMR with deuterated acetone d-6 (**Figure 14**). The NMR reveals a distinct peak at 0.06 ppm which would be the location of the trimethyl siloxane group.
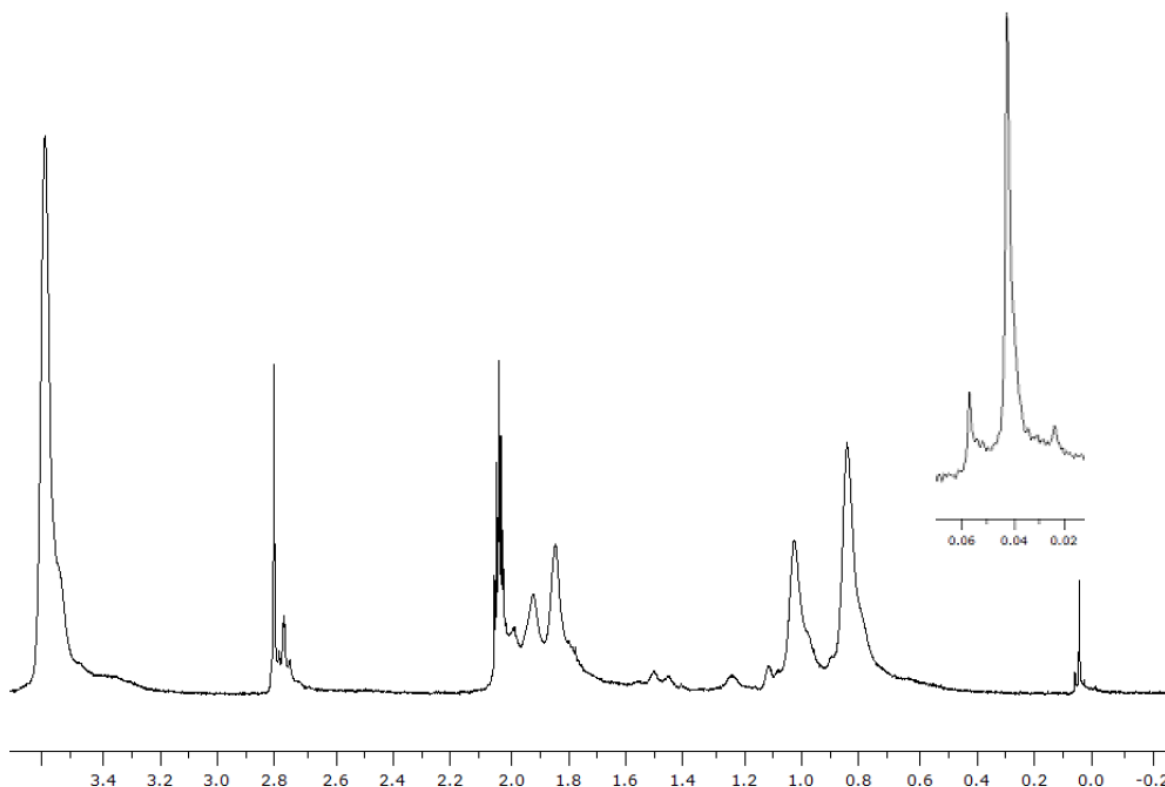
Figure 14: NMR of PMMA 4000

2.2.2 Analysis of PMMA 8000

Achieving a clean distribution of singly charged PMMA 4000 peaks, calculating end groups, and molecular weight distribution data was a good foundation for us to begin the analysis of the PMMA 8000 standard. The spectrum obtained below of PMMA 8000 is under optimized conditions without the addition of any cetyltrimethylammonium bromide (**Figure 15**).
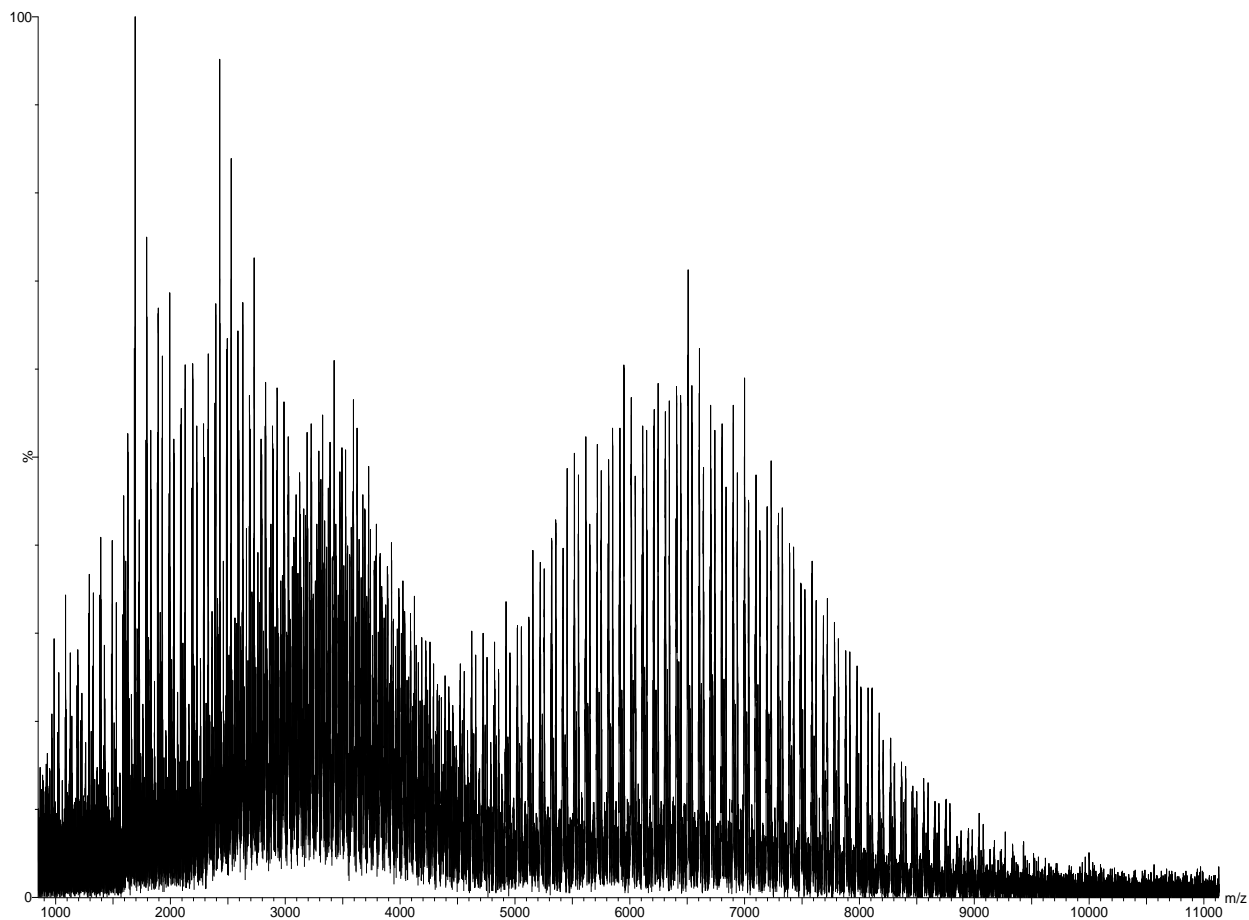
Figure 15: ESI-ToF of PMMA 8000 without a cationizing agent at optimized parameters

While Figure 15 does have a distribution of $[M + CTA]^+$ peaks present, it also contains a large amount of doubly and triply charged peaks; this creates a high degree of congestion in the lower m/z region. The high degree of congestion in this spectrum causes many lower intensity peaks to be lost in the baseline. Once again by simply adding cetyltrimethylammonium bromide and applying the optimized parameters we achieve a spectrum that is dominated by $[M + CTA]^+$ peaks (**Figure 16**).

31
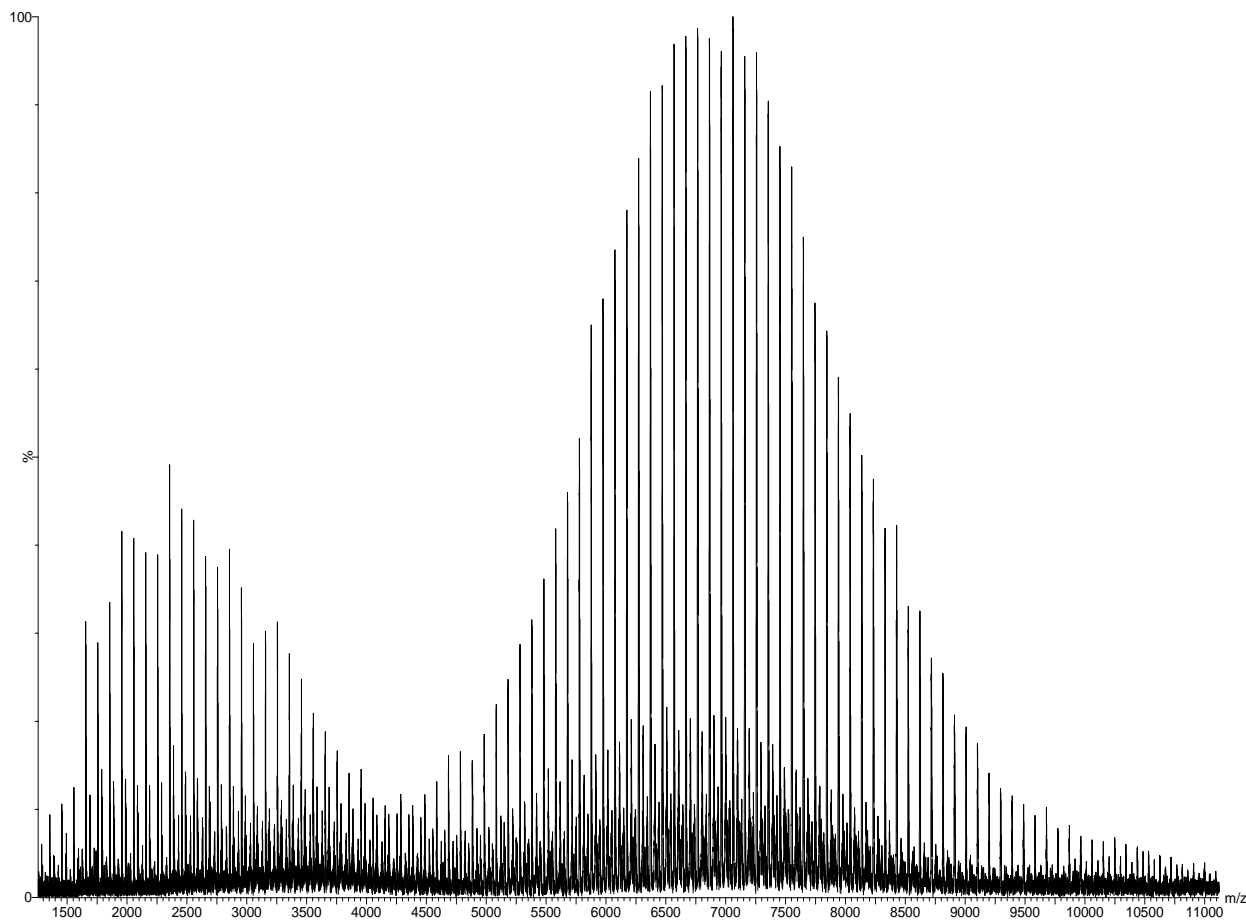
Figure 16: ESI-ToF of PMMA 8000 with the addition of cetyltrimethylammonium bromide under optimized conditions

There is a great improvement in the total ion intensity and $[M + CTA]^+$ from Figure 15 to Figure 16. It is also important to observe the peak distribution from approximately 1500 – 4000 m/z that was otherwise unobservable in Figure 15. As with PMMA 4000 the distribution of peaks present in PMMA 8000 are out of the calibration range and required a calibration correction. Table 6 is the mass to charge distribution of the species with the highest ion intensity present in the spectra.

Table 6: The actual m/z, intensity, and corrected m/z of PMMA 8000

Actual m/z	Intensity	Corrected m/z

32

3786.3394	7	3789.5697	7060.5718	66	7093.9298
3887.0732	7	3890.4449	7158.6260	63	7193.9035
3987.7104	7	3991.2877	7256.7622	63	7294.0451
4086.7490	6	4090.5861	7355.3721	60	7394.7571
4186.3916	6	4190.5428	7452.9805	56	7494.5340
4285.9800	8	4290.4942	7551.1987	55	7595.0245
4385.4707	7	4390.3934	7647.8760	50	7694.0284
4486.2681	8	4491.6487	7745.7559	45	7794.3566
4585.5786	9	4591.4519	7844.0933	43	7895.2493
4684.1055	11	4690.5070	7940.3237	39	7994.0746
4783.6821	11	4790.6563	8038.7891	36	8095.2932
4883.6821	10	4891.2704	8135.7378	33	8195.0510
4982.7236	12	4990.9587	8233.1807	31	8295.4171
5083.0117	15	5091.9412	8330.0869	28	8395.3307
5182.2583	16	5191.9148	8427.2529	28	8495.6141
5281.9390	19	5292.3667	8524.7606	22	8596.3539
5380.7715	21	5392.0057	8621.3428	21	8696.2413
5481.0098	24	5493.1061	8717.3691	18	8795.6574
5579.3418	28	5592.3289	8814.1387	17	8895.9489
5678.5386	30	5692.4714	8910.9443	14	8996.3853
5777.4741	34	5792.3995	9007.7813	13	9096.9632
5876.3735	43	5892.3425	9102.7256	12	9195.6827
5975.2876	45	5992.3543	9198.6904	9	9295.5727
6074.1943	49	6092.4147	9294.6016	8	9395.5185
6173.1943	52	6192.6284	9392.7490	8	9497.9119
6272.6221	56	6293.3370	9487.7734	7	9597.1623
6370.6284	60	6392.6689	9583.1211	6	9696.8661
6470.1416	61	6493.5948	9678.7402	7	9796.9725
6568.5918	64	6593.5113	9773.8955	5	9896.7140
6666.9492	65	6693.4045	9869.7207	5	9997.2821
6765.4272	65	6793.4935	9965.2939	5	10097.7132
6863.8550	65	6893.6072	10060.7432	4	10198.1445
6962.7705	63	6994.2957	10154.6200	4	10297.0519

The clean distribution of peaks from Figure 16 allows us to calculate the number average

molecular weight, weight average molecular weight, and polydispersity utilizing equations 1, 2,

and 3. Molecular weight distribution data from the ESI-ToF calculation, In-Lab GPC and

Manufacturer GPC can be found in Table 7.

Table 7: Molecular weight distribution data from ESI-ToF calculations, In-Lab GPC, and

Manufacturer GPC of PMMA 8000

Technique	M_w	M_n	PD
ESI - ToF	6915	6695	1.03
In-Lab GPC	6513	6183	1.05
Manufacturer GPC	7920	7950	1.04

The In-lab GPC values reveals that our percent difference of weight average molecular

weight from the ESI calculations is only 6.0%. Whereas the percent difference of weight average

molecular weight in the In-lab GPC values and ESI-ToF values from the manufacturer GPC

values are respectively 19.5% and 13.5%. As with the PMMA 4000 the In-Lab GPC's

calibration line was created with polystyrene standards, so a variation in molecular weight

calculation is possible when analyzing other polymers. The ESI-ToF calculations and the In-Lab

GPC results are in good correlation with one another.

The major species end groups have been determined to be two hydrogen's. The two

hydrogen end groups of the PMMA 8000 standard were confirmed by the manufacturer. A

summary of assigned structures to major peaks can be found in Table 8.

Table 8: PMMA 8000 Assigned Structures of Major Species

	m/z assignments	
Assigned Structure	[M+CTA]+	[M+Na]+

A   6293.3370   6231.2638

B   7168.1608   N/A

C   3658.7201   N/A
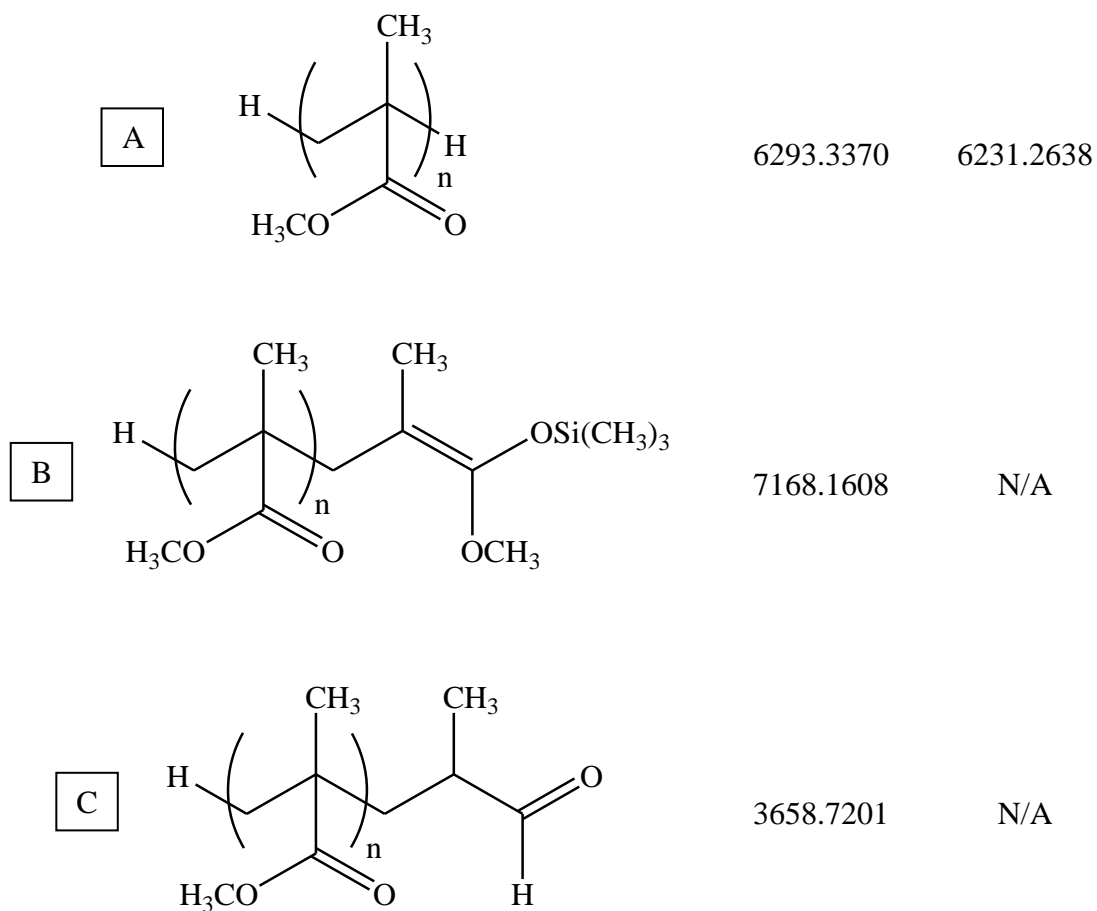
As with PMMA 4000 structure B and C is present in the ESI spectrum of PMMA 8000.
Once again we believe that the trimethylsilyl group is the cause of this fragmentation. A NMR
was run on PMMA 8000 with deuterated acetone d-6 to confirm that the trimethylsilyl was
present on the oligomer end group (**Figure 17**).
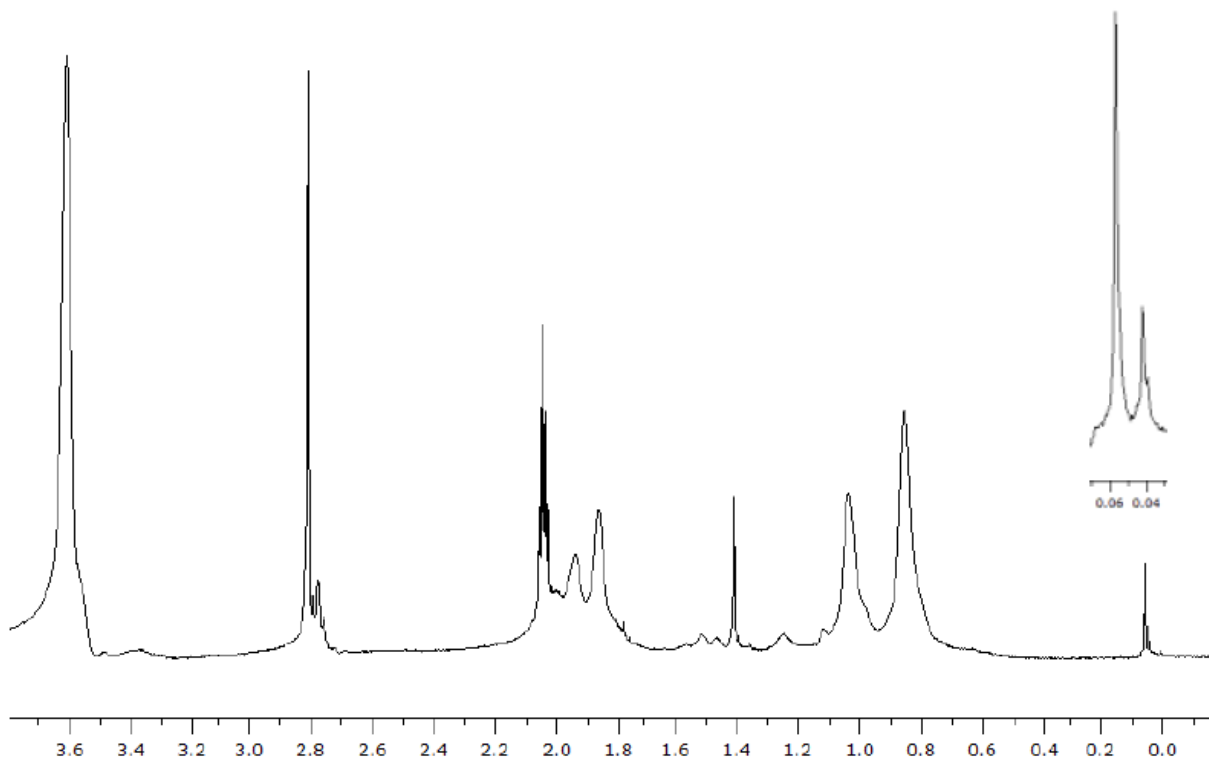
Figure 17: NMR of PMMA 8000

The NMR of PMMA 8000 reveals a very large peak present at 0.06 ppm which supports our conclusion that the trimethylsilyl group is present. The intensity of the 0.06 ppm peak is higher than that of the 0.6 ppm peak in PMMA 4000. This explains why we a higher abundance of structure C in the ESI spectrum.

2.2.3 Analysis of PMMA 12000

PMMA 12000 seemed to be an appropriate choice as the high end molecular weight standard that we wanted to analyze on our ESI-ToF. Our ESI-ToF has a limited mass to charge range in which it can analyze ions. This is just a software limitation and should not be thought of as an instrument issue. This standard was determined to have peaks that will extend approximately to the 17,000 m/z region, so it was within the appropriate range.

As with PMMA 4000 and 8000 the first task was analyzing PMMA 12,000 without the addition of any surfactant at optimized conditions. Figure 18 below is the prime spectrum obtained under optimized conditions.
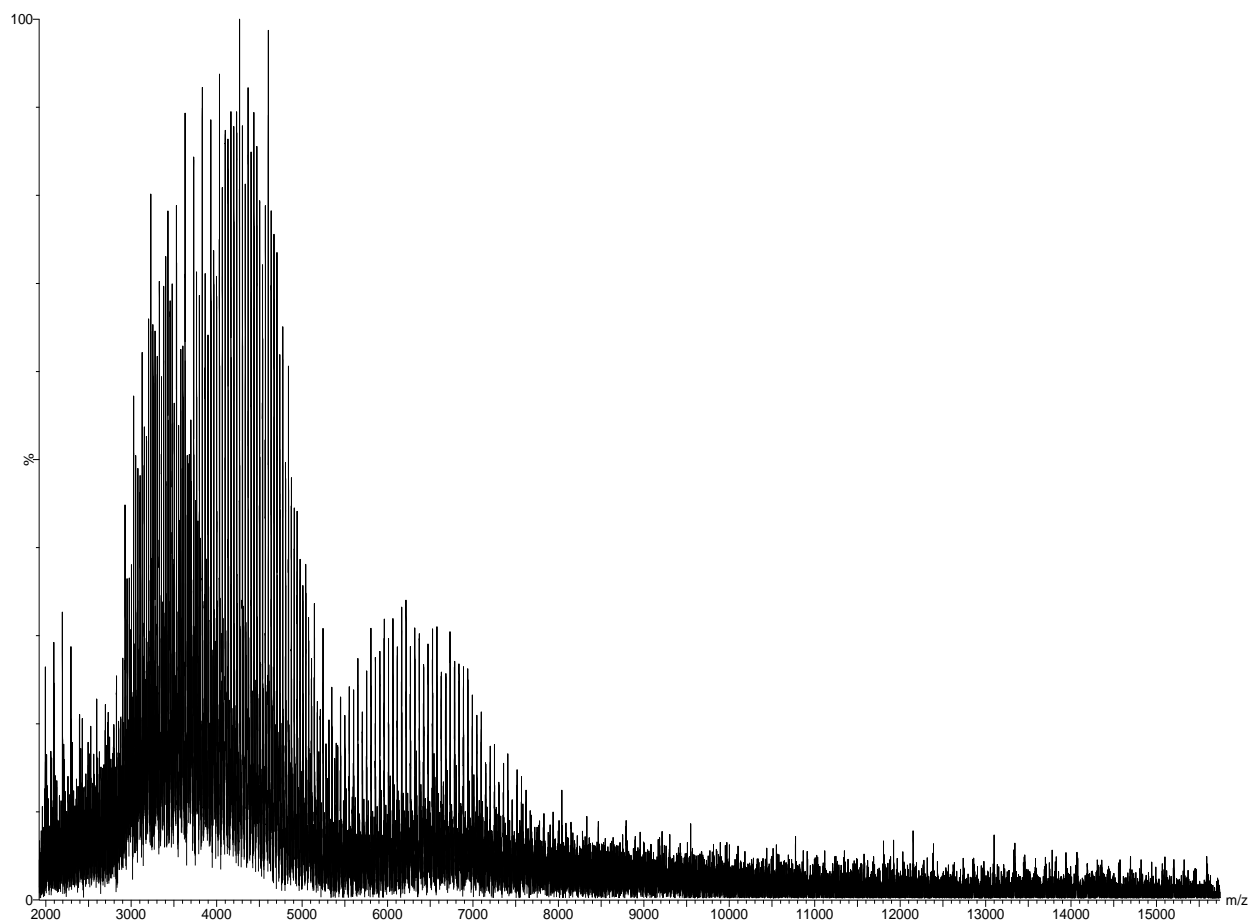
Figure 18: ESI-ToF of PMMA 12000 without a cationizing agent at optimized parameters

As you can see in Figure 18 there are little to no [M + Cation]$^+$ peaks present. However, there is a large abundance of doubly, triply and quadrupaly charged peaks which overlap one another. The addition of cetyltrimethylammonium bromide to the PMMA 12000 solution and applying the optimized parameters yielded Figure 19.
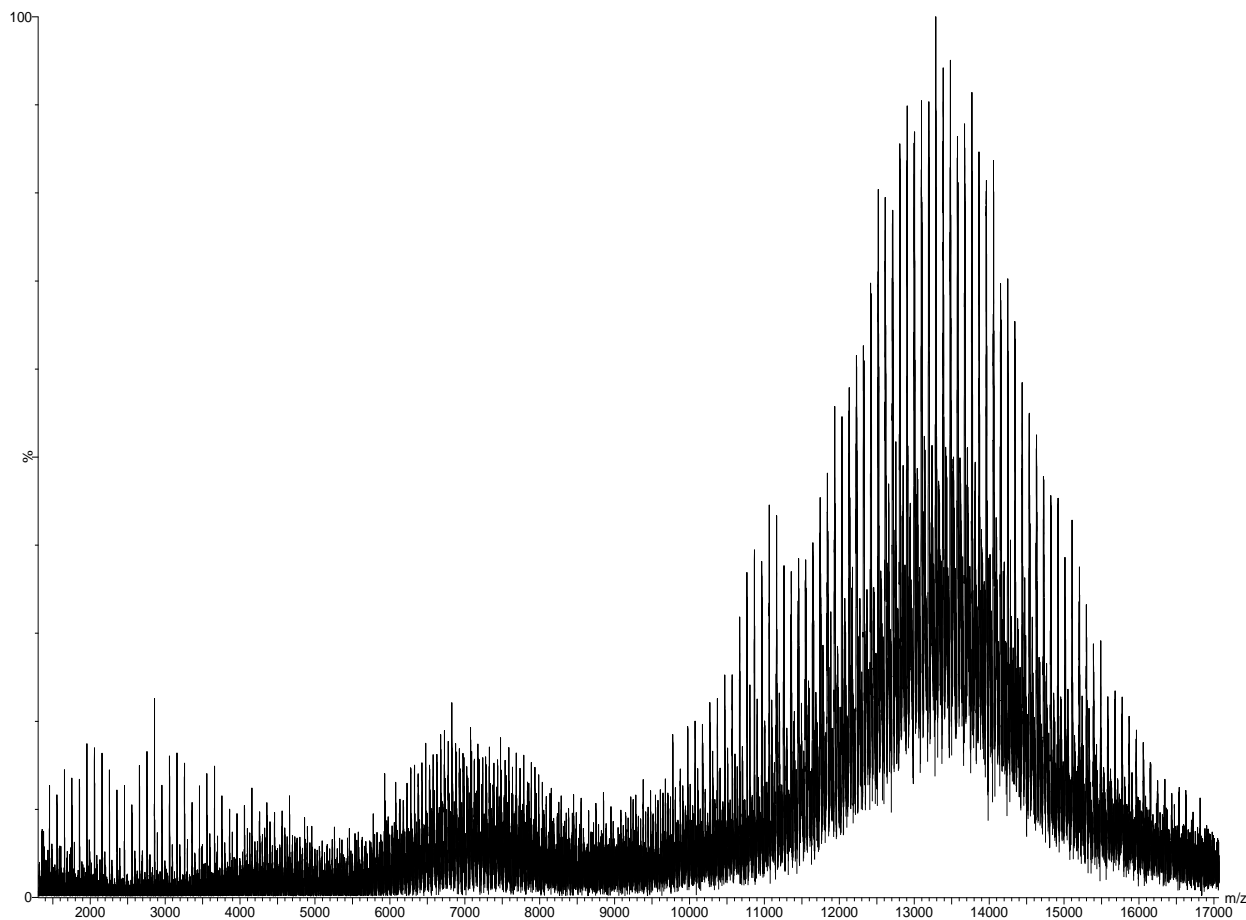
Figure 19: ESI-ToF of PMMA 12000 with the addition of cetyltrimethylammonium bromide under optimized conditions

The first thing to observe in Figure 19 is the $[M + Cation]^+$ region from approximately 1500 to 4000 m/z. This region was originally consumed by the triply and quadruply charged peaks which would otherwise be unobservable previously in Figure 18. While we were able to drastically reduce the multiply charged regions of PMMA 12000 with the addition of the surfactant we were unable to completely rid the spectrum of the doubly charged peaks. This is attributed to time constraints as well as issues with the ESI-ToF being unavailable. We are very confident that with further investigation we can improve the reduction of the intensity of the doubly charged peaks present. However the doubly charged peaks are diminished enough to be able to calculate molecular weight distribution data. Figure 20 is just an expansion of the [M +

CTA]$^+$ region to show the clean distribution of singly charged peaks. Figures 19 and 20 have been smoothed twice in order to reduce congestion.
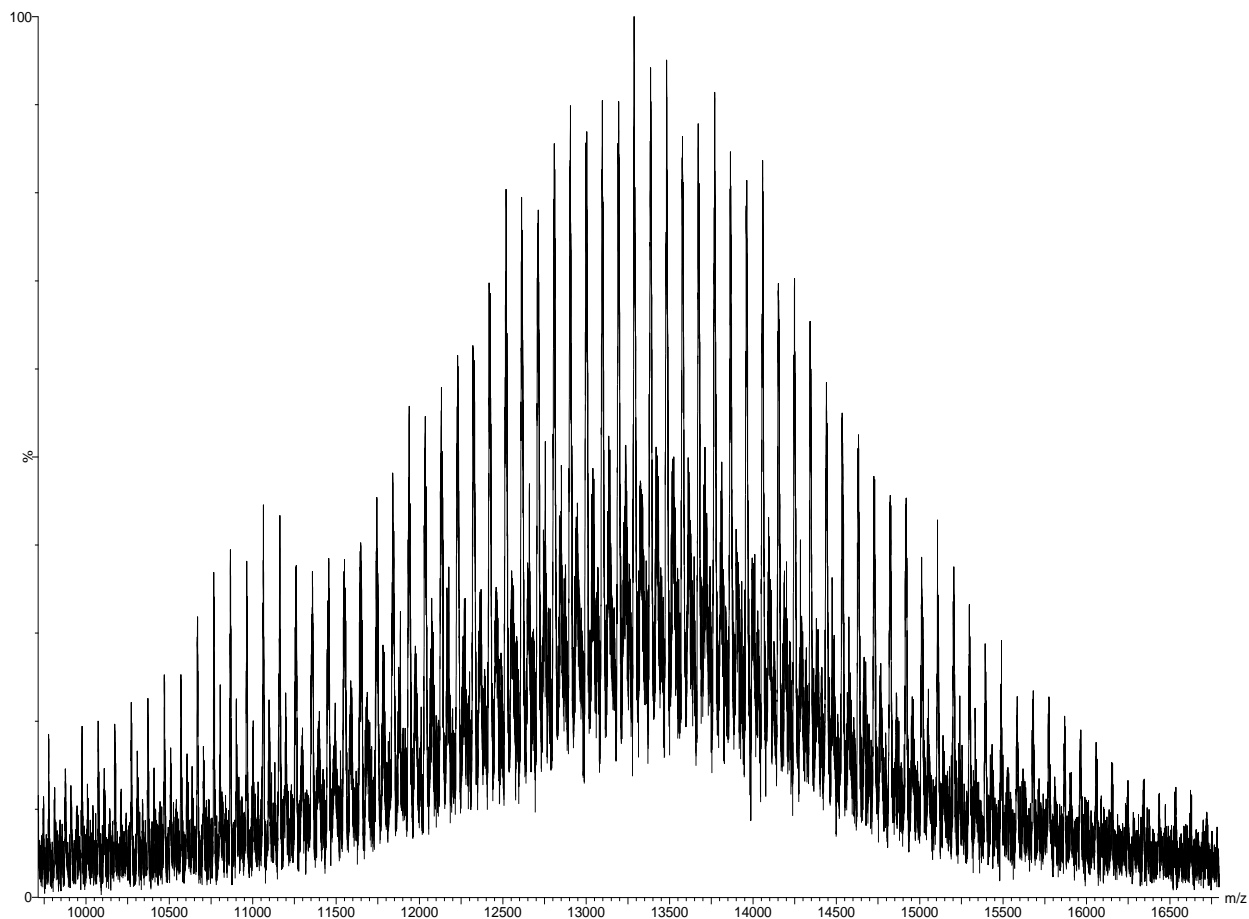
Figure 20: Expansion of the [M + CTA]$^+$ region from the ESI-ToF of PMMA 12000 with the addition of cetyltrimethylammonium bromide under optimized conditions

As with PMMA 4000 and 8000 the distribution of peaks present in PMMA 12000 are out the calibration range and required a calibration correction. An explanation for the ion intensity being low is that the [M + CTA]$^+$ species have such large masses and only one ion attached to them so it is difficult to focus them to the mass analyzer [22]. Table 9 is the distribution of the species with the highest ion intensity present in the spectra.

Table 9: The actual m/z, intensity, and corrected m/z of PMMA 12000

Actual m/z	Intensity	Corrected m/z			
10073.2734	3	10096.8808	13386.0879	13	13502.6375
10173.0986	3	10197.1250	13482.4160	13	13602.9588
10271.6924	3	10296.3185	13577.0693	12	13701.5705
10371.7588	3	10397.1873	13671.4072	12	13799.8898
10469.7402	3	10496.1464	13770.0713	12	13902.7589
10569.4805	3	10597.0777	13864.9375	11	14001.7105
10668.9746	4	10697.9553	13962.3145	11	14103.3272
10766.3818	5	10796.9037	14057.8096	11	14203.0288
10865.8936	5	10898.1764	14152.3555	9	14301.7902
10964.1865	5	10998.3884	14248.8047	10	14402.5952
11064.2451	6	11100.5776	14342.0430	9	14500.1007
11162.9160	6	11201.5174	14440.0346	8	14602.6399
11259.3652	5	11300.3379	14534.7988	7	14701.8662
11358.3799	5	11401.9366	14633.0400	7	14804.8024
11455.7588	5	11501.9964	14725.1797	6	14901.4113
11547.8457	5	11596.7379	14822.9220	6	15003.9654
11647.8701	5	11699.7686	14918.7314	6	15104.5626
11744.1172	6	11799.0208	15011.6279	5	15202.1680
11840.0557	6	11898.0560	15106.7266	6	15302.1537
11938.2744	7	11999.5415	15204.9063	5	15405.4461
12034.5693	7	12099.1259	15297.5605	4	15502.9837
12131.6367	8	12199.5886	15392.4814	4	15602.9606
12228.6406	8	12300.0580	15490.1494	4	15705.8788
12320.0410	9	12394.7839	15584.2793	3	15805.1048
12417.6719	9	12496.0257	15673.8467	3	15899.5437
12519.3125	11	12601.4837	15775.1787	3	16006.3980
12612.2764	11	12697.9865	15868.7197	3	16105.0299
12712.5469	11	12802.1202	15965.8486	3	16207.4176
12808.2441	12	12901.5454	16057.3701	2	16303.8472
12905.1728	12	13002.2881	16151.8838	2	16403.3564
13003.4092	12	13104.4267	16248.9385	2	16505.4335
13096.5029	12	13201.2508	16345.7510	2	16607.1125
13194.5117	12	13303.2205	16437.5430	2	16703.3507
13287.3398	14	13399.8315			

The distribution of peaks from Figure 20 allows us to calculate the number average molecular weight, weight average molecular weight, and polydispersity utilizing equations 1, 2, and 3. Molecular weight distribution data from the ESI-ToF calculation, In-Lab GPC and Manufacturer GPC can be found in Table 10.
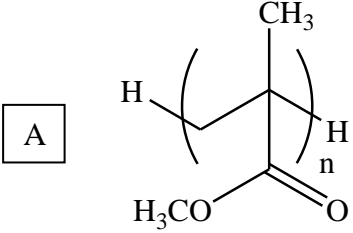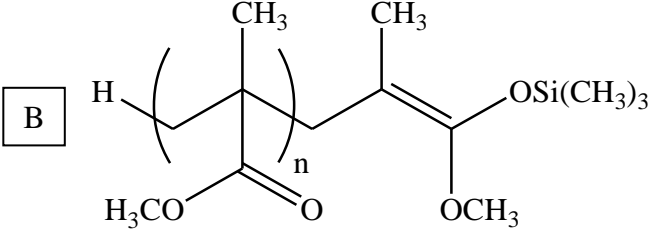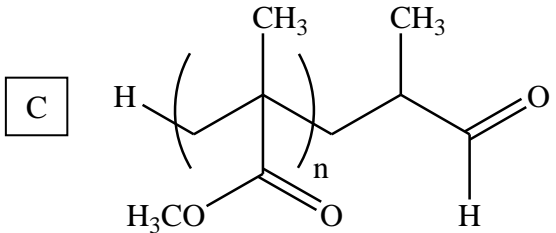
Table 10: Molecular weight distribution data from ESI-ToF calculations, In-Lab GPC, and Manufacturer GPC of PMMA 12000

Technique	M_w	M_n	PD
ESI - ToF	13150	12982	1.01
In-Lab GPC	12692	11987	1.06
Manufacturer GPC	12000	11540	1.04

The In-Lab GPC values reveals that our percent difference of weight average molecular weight from the ESI calculations is only 3.5%. Whereas the percent difference of weight average molecular weight in the GPC values and ESI values from the manufacturer values are respectively 5.6% and 9.1%. Further investigation of the PMMA 12000 is needed to fully elucidate the standard but current results seem very promising. The low ion abundance present could prove to be an issue with the molecular weight distribution calculations, but our calculations still seem to be in good correlation with one another. As with the PMMA 4000 and 8000 the In-Lab GPC's calibration line was created with polystyrene standards, so a variation in molecular weight calculation is possible when analyzing other polymers.

Table 11 is the assigned structures of the major species present in the ESI spectrum of PMMA 12000.

Table 11: PMMA 12000 Assigned Structures of Major Species

| | | m/z assignments | |
	Assigned Structure	[M+CTA]+	[M+Na]+
A		13399.8315	11637.8448
B		10470.4359	N/A
C		3057.1060	2796.0105

As with PMMA 4000 and 8000 we have come to the same conclusion with PMMA 12000 that structure C is a result of the fragmentation of the labile bond in structure B. The NMR of PMMA 12000 did not reveal trimethylsilyl group. However, this is not a surprise because as the molecular weight of the polymer grows the backbone concentration increases and the end group's concentration decreases. The concentration the trimethylsilyl end group appears to be so low that it is unobservable by NMR.

2.3 Surfactant Consideration

There are four different classes of surfactants which include cationic, anionic, zwitterion, and neutral. We are more interested in positive ion mode so using cationic surfactants is of greater significance in this case. Negative ion mode can be difficult because of possible occurrence of corona discharge. Corona discharge is an electrical discharge that occurs from the capillary tip that causes chemical ionization of solvent and gas phase analyte ions [33]. This tends to result in a significant amount of noise in the final spectrum. The surfactants that we have investigated are cetyltrimethylammonium bromide (**Figure 19**), dihexadecyldimethylammonium bromide (**Figure 20**), and tetrahexadecylammonium bromide (**Figure 21**). It is important to note that the surfactants only differ by the ligands that are attached to the nitrogen center atom. The manipulation of one variable would allow us to draw conclusions on the possible interactions of the polymer and the surfactant. Spectra as well as parameters can be found in Appendix D, E, and F.
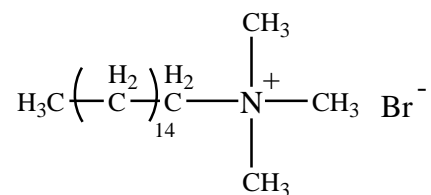
Figure 21: Cetyltrimethylammonium Bromide
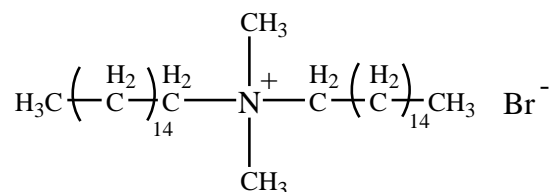
Figure 22: Dihexadecyldimethylammonium Bromide
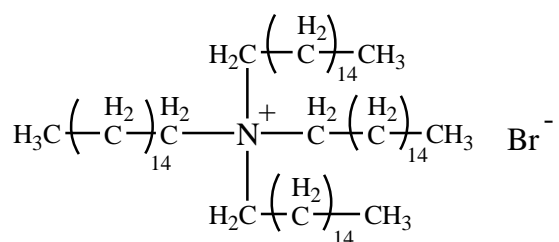
Figure 23: Tetrahexadecylammonium Bromide

While all of the surfactants reduced the $[M + 2Cation]^{2+}$ that took place with PMMA 4000 the ion intensity decreased with increasing surfactant bulkiness. Cetyltrimethylammonium bromide had the highest ion count of 203, while dihexadecyldimethylammonium bromide ion count was 157, and tetrahexadecylammonium bromide ion count was 88. This was attributed to a decline in the ability of the polymer and surfactant to form a stable interaction with increasing number of large ligands. While we are not certain about the actual mechanism of association between the polymer and the surfactant it is possible that during evaporation of the solvent from the final droplet the surfactant actually position itself onto the polymer before arriving to the gas phase.

2.4 Conclusion and Suggestions for Future Work

In conclusion this will be the first report detailing successful use of ESI-ToF to produce clean mass spectral data for PMMA with molecular weights > 3,000 g/mol. This was accomplished by utilizing cetyltrimethylammonium bromide and adjusting critical ESI parameters. We hypothesize that the parent and offspring droplets will have less cationizing agent because cetyltrimethylammonium ion is a great deal larger than other typical cationizing agents (i.e. Na^+) so less charge will be able to exist on the exterior of the droplet. The large surface area of the cetyltrimethylammonium ion will also hinder the polymers ability to gain multiple charges. The molecular weight data is in good agreement with In-lab GPC-MALS from 1,000 – 13,000 m/z (g/mol) with a percent difference of 6.6% for PMMA 4000, 6.0% for PMMA 8000, and 3.5% for PMMA 12000.

One of the long term goals of this project is to incorporate chromatographic separation, such as GPC. Addition of GPC would allow separation of highly complex mixtures prior to ESI-MS analysis. Also we could evaluate other surfactants and solvent systems. By creating a two part solvent system in which the core of the droplet is insoluble with the analyte and the outside of the solvent layer holds onto the analyte the offspring droplets will have predominately analyte present. Upon solvent evaporation from the final droplet more analyte will be ejected to the gas phase. A fluorinated surfactant could be of interest in analyzing a fluoropolymer. Typically fluropolymer's are not soluble in conventional ESI solvents; however the addition of a fluorinated surfactant may be able to bridge this gap by acting as a phase interface transferring agent. As stated earlier our ESI-ToF mass to charge range only extends to 20,000 m/z so using a surfactant with a higher charge state (i.e. +2, +3) could possibly control the charge state distribution. Controlling the charge state distribution could prove to be a valuable tool when

analyzing polymers which molecular weights which exceed the ESI-ToF mass to charge range.

Finally we plan on expanding this application to other synthetic polymers

CHAPTER 3: EXPERIMENTAL

3.1 Materials

The LC/UV grade acetone was manufactured by ChromAR (Lot number H14B00) and used without further alteration. The HPLC grade solvent tetrahydrofuran (THF) (Lot number G35804) was manufactured by J.T. Baker and used without further alteration. Anhydrous toluene (99.8%) was manufactured from Sigma Aldrich and used without further alteration.

Poly (methyl methacrylate) (PMMA) 4000 (Lot number WA22833) and 8000 (Lot number 0001428483) were purchased from Sigma Aldrich and were manufactured by Fluka utilizing group transfer polymerization. PMMA 12000 (Lot number 510978) was manufactured by Polymer Sciences Incorporated utilizing group transfer polymerization. Varian Incorporated polystyrene standards kit (Lot number 101) was manufactured by Polymer Labs and used without further alteration.

Cetyltrimethylammonium bromide (CTAB) (Lot number 116464641505047) was manufactured by Sigma and used without further alteration. Dihexadecyldimethylammonium bromide (Lot number 13813LH) and Tetrahexadecylammonium bromide (Lot number 04757811) were manufactured from Aldrich and were used without further alteration.

3.2 GPC Polystyrene Sample Preparation and Calibration

The following groups of polystyrene (PS) standards from Polymer Labs were added to three different 20 mL scintillation vials in preparation of GPC calibration. Vial one contained 0.0153 grams of PS 640, 0.0136 grams of PS 10290, 0.0113 grams of PS 200100, and 0.0051 grams of PS 2748000. Vial two contained 0.0158 grams of PS 1490, 0.0148 grams of PS 29460, and 0.0092 grams of PS 458700. Vial three contained 0.0148 grams of PS 3950, 0.0118 grams of

PS 69200, and 0.0061 grams of PS 1202000. Exactly 10.00 mL of THF was pipette into each scintillation vial. The solutions were allowed to sit for approximately one day before analysis. The columns were set in the following order: PLgel Mixed-C, PLgel Mixed-E, Waters HR 2, and Waters HR 0.5. Distribution data was extracted from Millennium and imported to Cirrus in order to create the calibration curve.

3.2.1 PMMA Standard Sample Preparation and Analysis for GPC

0.0051 grams of PMMA 4000 was added to a 20 mL scintillation vial followed by 1.5 mL of THF. The sample was then spiked with 2 µM of toluene. 0.0047 grams of PMMA 8000 was added to a 20 mL scintillation vial followed by 1.5 mL of THF. The sample was then spiked with 2 µM of toluene. 0.0051 grams of PMMA 12000 was added to a 20 mL scintillation vial followed by 1.5 mL of THF. The sample was then spiked with 2 µM of toluene. The solutions were allowed to sit for approximately one day before analysis. Distribution data was extracted from Millennium and imported to Cirrus. Molecular weight data from each run was calculated using the calibration line created from the PS standards.

3.3 ESI-ToF Sample Preparation

0.0041 g of the Sigma cetyltrimethylammonium bromide (CTAB) surfactant was added to a 20 mL scintillation vial followed by 20.00 mL of LC/UV grade acetone. The solution was stored in a lab drawer until necessary for ESI-ToF analysis.

0.0109 g of the Fluka PMMA 4000 standard was added to a 20 mL scintillation vial followed by the addition of 20.00 mL of LC/UV grade acetone. The standard was stored in a lab drawer until ESI-ToF analysis. Prior to ESI analysis 40.0 µL of the solution was transferred to a

20 mL scintillation vial followed by the addition 70.0 µL of the CTAB solution. 10.00 mL of the LC/UV grade acetone was then added to the scintillation vial.

0.0202 g of the Fluka PMMA 8000 standard was added to a 20 mL scintillation vial followed by the addition of 20.00 mL of LC/UV grade acetone. The standard was stored in a lab drawer until ESI-ToF analysis. Prior to ESI analysis 150.0 µL of the solution was transferred to a 20 mL scintillation vial followed by the addition of 40.0 µL of the CTAB solution. 10.00 mL of the LC/UV grade acetone was then added to the scintillation vial.

0.0255 g of the Polymer Sciences PMMA 12000 standard was added to a 20 mL scintillation vial followed by the addition of 20.00 mL of LC/UV grade acetone. The standard was stored in a lab drawer until ESI-ToF analysis. Prior to ESI analysis 50.0 µL of the solution was transferred to a 20 mL scintillation vial followed by the addition of 30.0 µL of the CTAB solution. 10.00 mL of the LC/UV grade acetone was then added to the scintillation vial.

0.0044 g of the Aldrich dihexadecyldimethylammonium bromide surfactant was added to a 20 mL scintillation vial followed by 20.00 mL of LC/UV grade acetone. The solution was stored in a lab drawer until necessary ESI-ToF analysis. Prior to ESI analysis 45.0 µL of the PMMA solution was transferred to a 20 mL scintillation vial followed by the addition of 26.6 µL of the dihexadecyldimethylammonium bromide solution. 10.00 mL of the LC/UV grade acetone was then added to the scintillation vial.

0.0045 g of the Sigma tetrahexadecylammonium bromide surfactant was added to a 20 mL scintillation vial followed by 20.00 mL of LC/UV grade acetone. The solution was stored in a lab drawer until necessary ESI-ToF analysis. Prior to ESI analysis 45.0 µL of the PMMA solution was transferred to a 20 mL scintillation vial followed by the addition of 26.6 µL of the

tetrahexadecylammonium bromide solution. 10.00 mL of the LC/UV grade acetone was then

added to the scintillation vial.

3.3.2 ESI Parameters for Each Sample

PMMA 4000 spectrum without CTAB (**Figure 11**) had the following ES parameters applied:

Parameter	Setting
Capillary Voltage	2900
Sample Cone Voltage	100
Extraction Cone Voltage	2.0
Source Temperature (°C)	90
Desolvation Temperature (°C)	150
Cone Gas Flow Rate (L/hr)	0
Desolvation Gas Flow Rate (L/hr)	500
Syringe Pump Flow Rate (µL/min)	5.0

Analysis Time – 5 minutes

PMMA 4000 with CTAB (**Figure 12**) had the following ES parameters applied:

Parameter	Setting
Capillary Voltage	2900
Sample Cone Voltage	100
Extraction Cone Voltage	2.0
Source Temperature (°C)	90
Desolvation Temperature (°C)	150
Cone Gas Flow Rate (L/hr)	0
Desolvation Gas Flow Rate (L/hr)	500
Syringe Pump Flow Rate (µL/min)	5.0

Analysis Time – 5 minutes

PMMA 8000 without CTAB (**Figure 14**) had the following ES parameters applied:

Parameter	Setting
Capillary Voltage	2900
Sample Cone Voltage	140
Extraction Cone Voltage	2.0
Source Temperature (°C)	90

Parameter	Setting
Desolvation Temperature (°C)	150
Cone Gas Flow Rate (L/hr)	0
Desolvation Gas Flow Rate (L/hr)	500
Syringe Pump Flow Rate (µL/min)	10.0

Analysis Time – 6 minutes

Smoothing

    Smooth window (channels) – 3

    Number of smooths – 2

PMMA 8000 with CTAB (**Figure 15**) had the following ES parameters applied:

Parameter	Setting
Capillary Voltage	2900
Sample Cone Voltage	140
Extraction Cone Voltage	2.0
Source Temperature (°C)	90
Desolvation Temperature (°C)	140
Cone Gas Flow Rate (L/hr)	0
Desolvation Gas Flow Rate (L/hr)	500
Syringe Pump Flow Rate (µL/min)	10.0

Analysis Time – 6 minutes

Smoothing

    Smooth window (channels) – 3

    Number of smooths – 2

PMMA 12000 without CTAB (**Figure 16**) had the following ES parameters applied:

Parameter	Setting
Capillary Voltage	2900
Sample Cone Voltage	150
Extraction Cone Voltage	2.0
Source Temperature (°C)	90
Desolvation Temperature (°C)	150
Cone Gas Flow Rate (L/hr)	0
Desolvation Gas Flow Rate (L/hr)	500

Analysis Time – 10 minutes

Smoothing

Smooth window (channels) – 3

Number of smooths – 4

PMMA 12000 with CTAB (**Figure 17**) had the following ES parameters applied:

Parameter	Setting
Capillary Voltage	2900
Sample Cone Voltage	150
Extraction Cone Voltage	2.0
Source Temperature (°C)	90
Desolvation Temperature (°C)	150
Cone Gas Flow Rate (L/hr)	0
Desolvation Gas Flow Rate (L/hr)	500
Syringe Pump Flow Rate (μL/min)	10.0

Analysis Time – 10 minutes

Smoothing

Smooth window (channels) – 3

Number of smooths – 4

3.4 NMR Sample Preparation

0.0055 grams of PMMA 4000 was added to a GPC vial followed by 1.00 mL of deuterated acetone d-6. The solution was then transferred to a NMR tube followed by approximately a drop of acetone d-6 that contained 0.03% TMS. The above procedure was duplicated with 0.0059 g of PMMA 8000 and 0.0124 g of PMMA 12000. The samples were run on a 300 MHz NMR.

REFERENCES

1.   Flory, P.J., *Principles of Polymer Chemistry* 1953, Ithaca, N.Y.: Cornell University Press.

2.   Goodyear, C., *Improvement In India-Rubber Fabrics*. 1844.

3.   Baekeland, L.H., *Synthesis of condensation product of phenols and formaldehyde*. 1908.

4.   Staudinger, H., *Polymerization.* Berichte der Deutschen Chemischen Gesellschaft [Abteilung] B: Abhandlungen, 1920. **53B**: p. 1073-1085.

5.   Jiang, X., et al., *Mass Spectrometric Characterization of Functional Poly(methyl methacrylate) in Combination with Critical Liquid Chromatography* Analytical Chemistry, 2003. **75**(20): p. 5517-5524.

6.   Jackson, A.T., et al., *Characterization of end groups in poly(2-hydroxyethyl methacrylate) by means of electrospray ionization-mass spectrometry/mass spectrometry (ESI-MS/MS)* Polymer, 2010. **51**(6): p. 1418-1424.

7.   Romack, T.J., et al., *Characterization of perfluoroalkyl acrylic oligomers by electrospray ionization time-of-flight mass spectrometry* Rapid Communications in Mass Spectrometry, 2008. **22**(7): p. 930-934.

8.   Murgasova, R. and D.M. Hercules, *Polymer characterization by combining liquid chromatography with MALDI and ESI mass spectrometry* Analytical and Bioanalytical Chemistry, 2002. **373**(6): p. 481-489.

9.   Dole, M., et al., *Molecular beams of macroions.* Journal of Chemical Physics, 1968. **49**(5): p. 2240-2249.

10.   Fenn, J.B. and M. Yamashita, *Electrospray ion source. Another variation on the free-jet theme* Journal of Physical Chemistry, 1984. **88**(20): p. 4451-4459.

11.   Tanaka, K., et al., *Protein and polymer analyses up to m/z 100,000 by laser ionization time-of-flight mass spectrometry* Rapid Communications in Mass Spectrometry, 1988. **2**(8): p. 151-153.

12.   Crews, P., J. Rodriguez, and M. Jaspars, *Organic Structure Analysis*. Topics In Organic Chemistry, ed. K. Houk. 1998, New York: Oxford University Press.

13.   Iribarne, J.V. and B.A. Thomson, *On the evaporation of small ions from charged droplets.* Journal of Chemical Physics, 1976. **64**(6): p. 2287-2294.

14.   Kebarle, P., *A brief overview of the present status of the mechanisms involved in electrospray mass spectrometry.* Journal of Mass Spectrometry, 2000. **35**: p. 804-817.

15.   Rayleigh, L., Philos. Mag., 1882. **49**: p. 2240.

16.   Cole, R.B. and G. Wang, *Effects of solvent and counterion on ion pairing and observed charge states of diquaternary ammonium salts in electrospray ionization mass spectrometry* Journal of the American Society for Mass Spectrometry, 1996. **7**(10): p. 1050-1058.

17.   Iavarone, A.T. and E.R. Williams, *Mechanism of Charging and Supercharging Molecules in Electrospray Ionization* Journal of the American Chemical Society, 2003. **125**(8): p. 2319-2327.

18.   Sherman, C.L. and J.S. Brodbelt, *An equilibrium partitioning model for predicting response to host-guest complexation in electrospray ionization mass spectrometry* Analytical chemistry, 2003. **75**(8): p. 1828-1836.

19.   Cech, N.B. and C.G. Enke, *Relating Electrospray Ionization Response to Nonpolar Character of Small Peptides.* Analytical Chemistry, 2000. **72**(13): p. 2717-2723.

20.   Tang, K. and R.D. Smith, *Physical/chemical separations in the break-up of highly charged droplets from electrosprays* Journal of the American Society for Mass Spectrometry, 2001. **12**(3): p. 343-347.

21.   Grimm, R.L. and J.L. Beauchamp, *Evaporation and Discharge Dynamics of Highly Charged Droplets of Heptane, Octane, and p-Xylene Generated by Electrospray Ionization.* Analytical Chemistry, 2002. **74**(24): p. 6291-6297.

22.   Hunt, S.M., et al., *Probing the Effects of Cone Potential in the Electrospray Ion Source: Consequences for the Determination of Molecular Weight Distributions of Synthetic Polymers* Analytical Chemistry, 1998. **70**(9): p. 1812-1822.

23.   Kehr, S. and H. Luftmann, *Polymer characterization by electrospray-mass-spectrometry - shifting the upper mass limit* e-Polymers, 2007.

24.   Touboul, D., M.C. Jecklin, and R. Zenobi, *Ion internal energy distributions validate the charge residue model for small molecule ion formation by spray methods* Rapid Communications in Mass Spectrometry, 2008. **22**(7): p. 1062-1068.

25.   Fenn, J.B., *Ion formation from charged droplets: roles of geometry, energy, and time* Journal of the American Society for Mass Spectrometry, 1993. **4**(7): p. 524-535.

26.   Fenn, J.B. and T. Nohmi, *Electrospray mass spectrometry of poly(ethylene glycols) with molecular weights up to five million.* Journal of the American Chemical Society, 1992. **114**(9): p. 3241-3246.

27.   Enke, C.G., *A predictive model for matrix and analyte effects in electrospray ionization of singly-charged ionic analytes* Analytical Chemistry, 1997. **69**(23): p. 4885-4893.

28.   Waters, *Micromass Q-Tof micro Mass Spectrometer Operator's Guide*. 2002.

29.   Bahadur, P. and N.V. Sastry, *Principles of Polymer Science*. 2002, New Dehli: Narosa Publishing House.

30.   Webster, O.W., et al., *Group-transfer polymerization. 1. A new concept for addition polymerization with organosilicon initiators* Journal of the American Chemical Society, 1983. **105**(17): p. 5706-5708.

31.   Raynaud, J., Y. Gnanou, and D. Taton, *Group Transfer Polymerization of (Meth)acrylic Monomers Catalyzed by N-Heterocyclic Carbenes and Synthesis of All Acrylic Block Copolymers: Evidence for an Associative Mechanism* Macromolecules, 2009. **42**(16): p. 5996-6005.

32.   Scholten, M.D., J.L. Hedrick, and R.M. Waymouth, *Group Transfer Polymerization of Acrylates Catalyzed by N-Heterocyclic Carbenes*. Macromolecules, 2008. **41**(20): p. 7399-7404.

33.   Kebarle, P. and H. Yeunghaw, eds. *On the mechanism of electrospray mass spectrometry*. Electrospray Ionization Mass Spectrometry, ed. R.B. Cole. 1997, Wiley: New York. 3-63.

APPENDIX A. Calibration of PMMA 4000.

Calculated ESI Peaks of PMMA 4000 with two hydrogen end groups with CTAB as the cationizing agent

n	m/z
1	386.3998
10	1286.8717
20	2288.3994
30	3289.9270
40	4290.4512
50	5291.9790
60	6293.5063
70	7294.0308
80	8295.5586
90	9296.0830
100	10297.6104

Actual Collected ESI Data of PMMA 4000

n	m/z
10	1387.0931
11	1487.1329
12	1588.1923
13	1688.2686
14	1788.3169
15	1888.3674
16	1988.3804
17	2088.4080
18	2188.4202
19	2288.4287
20	2388.3948
21	2488.3406
22	2588.2805
23	2688.1929
24	2788.0654
25	2887.8955
26	2987.4190
27	3087.5149
28	3187.2622
29	3286.9307

30	3387.6172
31	3487.1968
32	3586.7632
33	3686.2539
34	3785.6951
35	3885.0593
36	3984.3513
37	4083.6096
38	4182.7554
39	4281.8633
40	4380.8257
41	4479.7881
42	4579.5825
43	4678.3066
44	4775.9565
45	4875.5557
46	4974.0425
47	5072.1992
48	5169.6133
49	5268.5703
50	5366.6226
51	5464.6636
52	5561.9966
53	5659.5723
54	5756.2295
55	5854.2622
56	5952.5537
57	6049.7388
58	6145.5884
59	6243.1260
60	6339.5972
61	6437.2598
62	6532.5767
63	6628.0586

Linear trendline of the calculated ESI data – $y = 9.98854E\text{-}03x_c - 2.85816$

6th order polynomial trendline of the actual ESI data – $y = 1.15827E\text{-}22x_a{}^6 - 2.90130E\text{-}18x_a{}^5 + 2.92418E\text{-}14x_a{}^4 - 1.44442E\text{-}10x_a{}^3 + 3.77375E\text{-}07x_a{}^2 + 9.49660E\text{-}03x_a - 2.61286$

Equations set equal and solved for x_c -

$x_c = (1.15827E\text{-}22x_a{}^6 - 2.90130E\text{-}18x_a{}^5 + 2.92418E\text{-}14x_a{}^4 - 1.44442E\text{-}10x_a{}^3 + 3.77375E\text{-}07x_a{}^2 + 9.49660E\text{-}03x_a + 0.24530) / 9.98854E\text{-}03$

APPENDIX B. Calibration of PMMA 8000.

Calculated ESI Peaks of PMMA 8000 with two hydrogen end groups with CTAB as the cationizing agent

n	m/z
1	386.3998
10	1286.8717
20	2288.3994
30	3289.9270
40	4290.4512
50	5291.9790
60	6293.5063
70	7294.0308
80	8295.5586
90	9296.0830
100	10297.6104

Actual Collected ESI Data of PMMA 8000

n	m/z
10	1387.0931
11	1487.1329
12	1588.1923
13	1688.2686
14	1788.3169
15	1888.3674
16	1988.3804
17	2088.4080
18	2188.4202
19	2288.4287
20	2388.3948
21	2488.3406
22	2588.2805
23	2688.1929
24	2788.0654
25	2887.8955
26	2987.4190
27	3087.5149
28	3187.2622
29	3286.9307

30	3387.6172
31	3487.1968
32	3586.7632
33	3686.2539
34	3785.6951
35	3885.0593
36	3984.3513
37	4083.6096
38	4182.7554
39	4281.8633
40	4380.8257
41	4479.7881
42	4579.5825
43	4678.3066
44	4775.9565
45	4875.5557
46	4974.0425
47	5072.1992
48	5169.6133
49	5268.5703
50	5366.6226
51	5464.6636
52	5561.9966
53	5659.5723
54	5756.2295
55	5854.2622
56	5952.5537
57	6049.7388
58	6145.5884
59	6243.1260
60	6339.5972
61	6437.2598
62	6532.5767
63	6628.0586

Linear trendline of the calculated data – $y = 9.98854E-03x_c - 2.85816$

6th order polynomial trendline of the actual ESI data – $y = 2.13185E-23x_a{}^6 - 9.45430E-19x_a{}^5 + 1.70983E-14x_a{}^4 - 1.57815E-10x_a{}^3 + 8.04178E-07x_a{}^2 + 7.85639E-03x_a - 5.56546E-01$

Equations set equal and solved for x_c -

$x_c = (2.13185E-23x_a{}^6 - 9.45430E-19x_a{}^5 + 1.70983E-14x_a{}^4 - 1.57815E-10x_a{}^3 + 8.04178E-07x_a{}^2 + 7.85639E-03x_a + 2.3016) / 9.98854E-03$

APPENDIX C. Calibration of PMMA 12000.

Calculated ESI Peaks of PMMA 12000 with two hydrogen end groups with CTAB as the cationizing agent

n	m/z
60	6293.5063
70	7294.0308
80	8295.5586
90	9296.0830
100	10297.6104
110	11299.1377
120	12299.6621
130	13301.1895
140	14302.717
150	15303.241
160	16304.769
170	17306.297
180	18306.82
190	19308.348

Actual Collected ESI Data of PMMA 12000

n	m/z
99	10173.0986
100	10271.6924
101	10371.7588
102	10469.7402
103	10569.4805
104	10668.9746
105	10766.3818
106	10865.8936
107	10964.1865
108	11064.2451
109	11162.9160
110	11259.3652
111	11358.3799
112	11455.7588
113	11547.8457
114	11647.8701
115	11744.1172

116	11840.0557
117	11938.2744
118	12034.5693
119	12131.6367
120	12228.6406
121	12320.0410
122	12417.6719
123	12519.3125
124	12612.2764
125	12712.5469
126	12808.2441
127	12905.1728
128	13003.4092
129	13096.5029
130	13194.5117
131	13287.3398
132	13386.0879
133	13482.4160
134	13577.0693
135	13671.4072
136	13770.0713
137	13864.9375
138	13962.3145
139	14057.8096
140	14152.3555
141	14248.8047
142	14342.0430
143	14440.0346
144	14534.7988
145	14633.0400
146	14725.1797
147	14822.9220
148	14918.7314
149	15011.6279
150	15106.7266
151	15204.9063
152	15297.5605
153	15392.4814
154	15490.1494
155	15584.2793
156	15673.8467

157	15775.1787
158	15868.7197
159	15965.8486
160	16057.3701
161	16151.8838
162	16248.9385
163	16345.7510
164	16437.5430
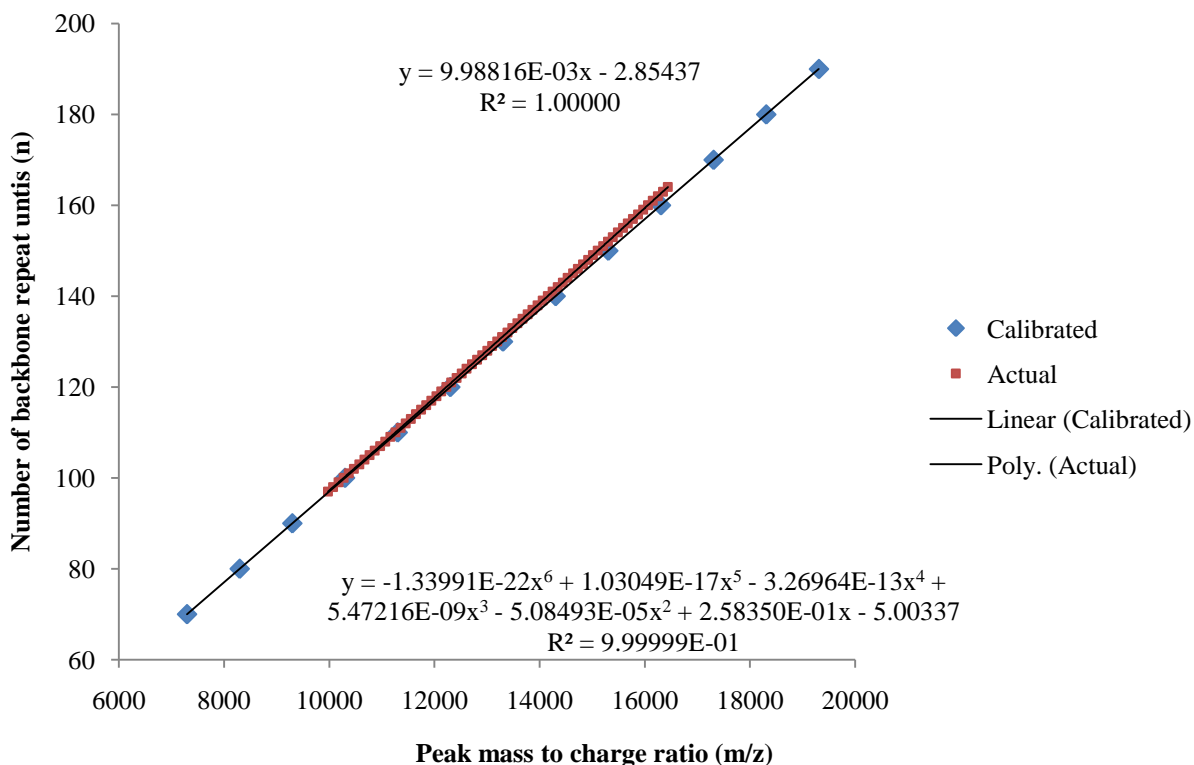
Linear trendline of the calculated ESI data – $y = 9.98816\text{E-}03x_c - 2.85437$

6th order polynomial trendline of the actual ESI data – $y = -1.33991\text{E-}22x_a^6 + 1.03049\text{E-}17x_a^5 - 3.26964\text{E-}13x_a^4 + 5.47216\text{E-}09x_a^3 - 5.08493\text{E-}05x_a^2 + 2.58350\text{E-}01x_a - 5.00337\text{E+}02$

Equations set equal and solved for x_c -

$x_c = (-1.33991\text{E-}22x_a^6 + 1.03049\text{E-}17x_a^5 - 3.26964\text{E-}13x_a^4 + 5.47216\text{E-}09x_a^3 - 5.08493\text{E-}05x_a^2 + 2.58350\text{E-}01x_a + 4.9748\text{E+}2) / 9.98816\text{E-}03$

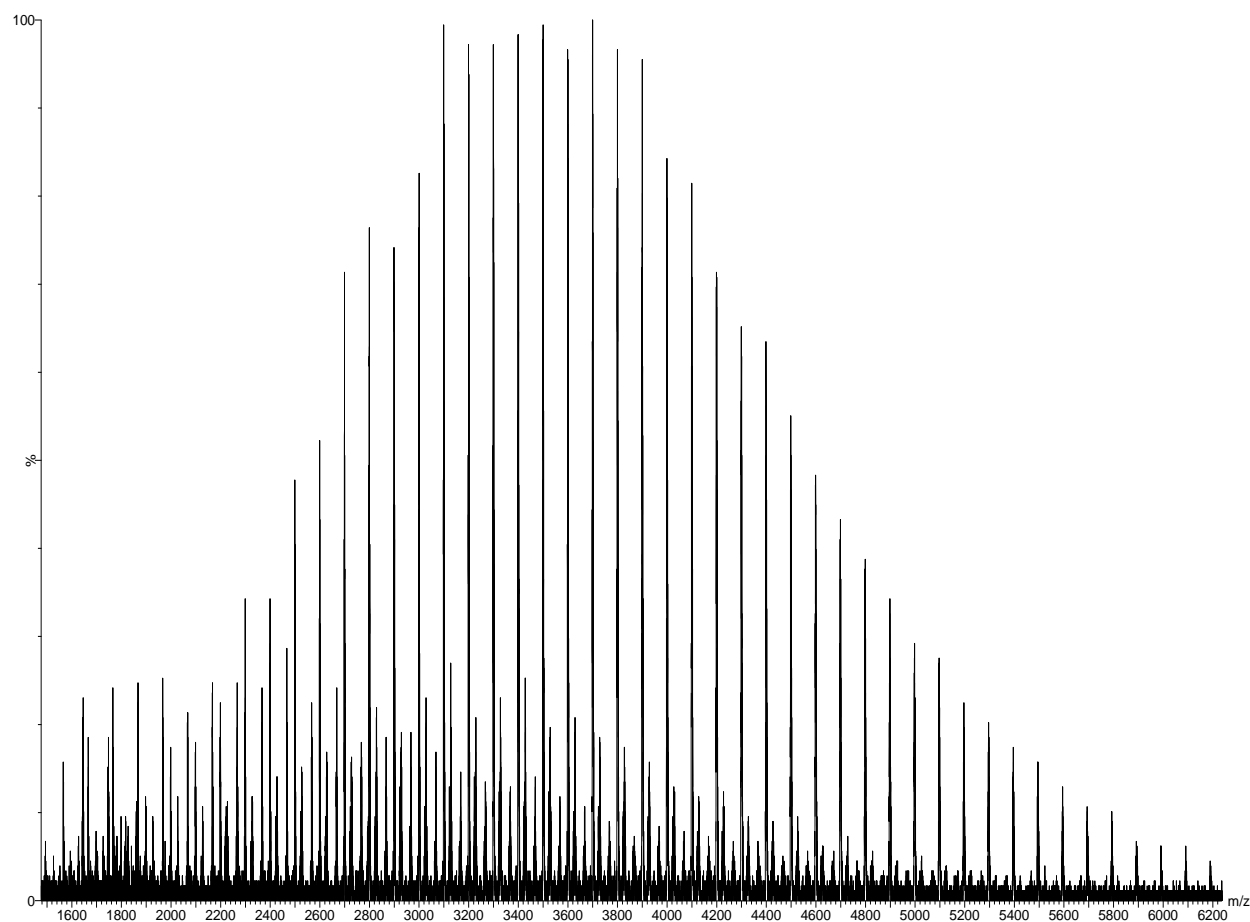APPENDIX D. Spectrum and Parameters of PMMA 4000 with Cetyltrimethylammonium
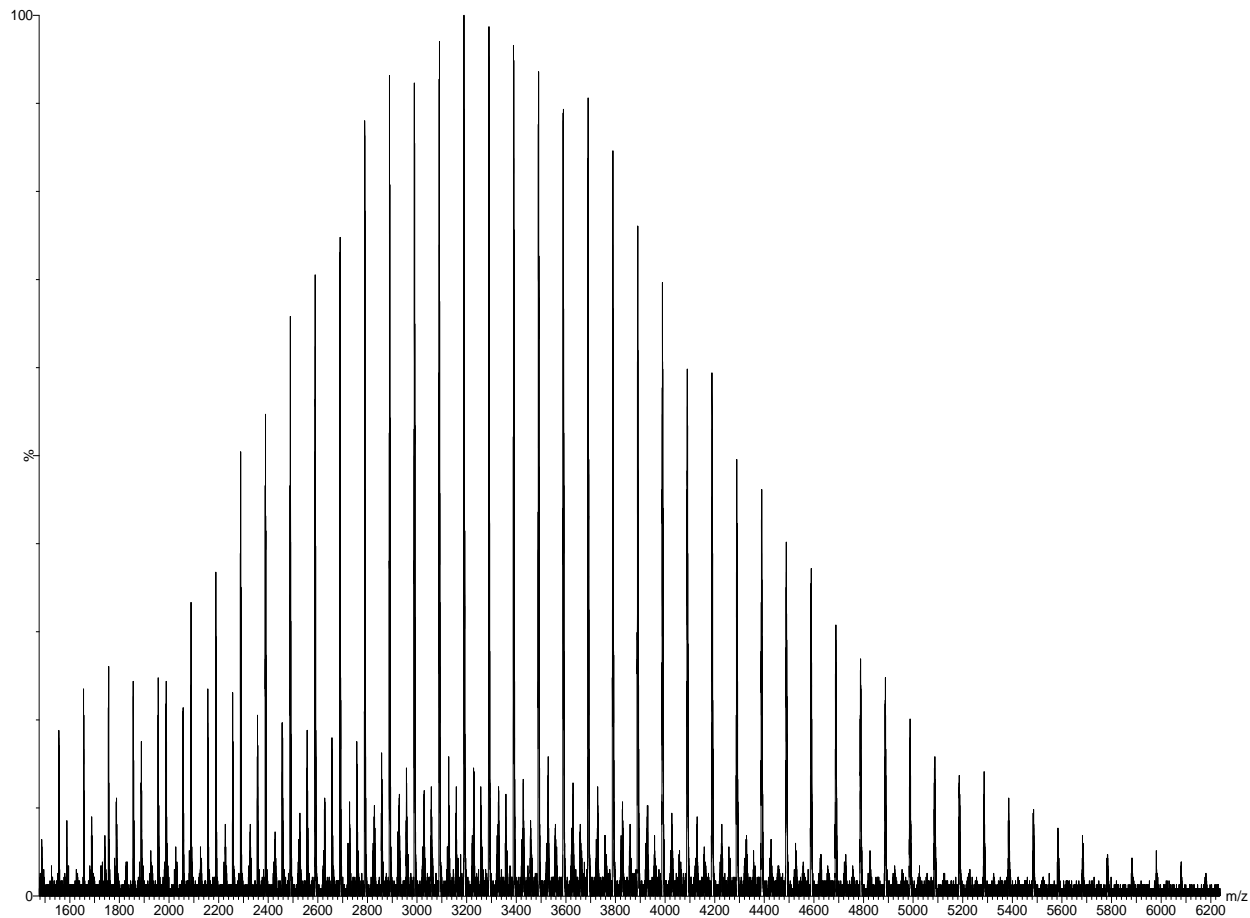
Bromide.

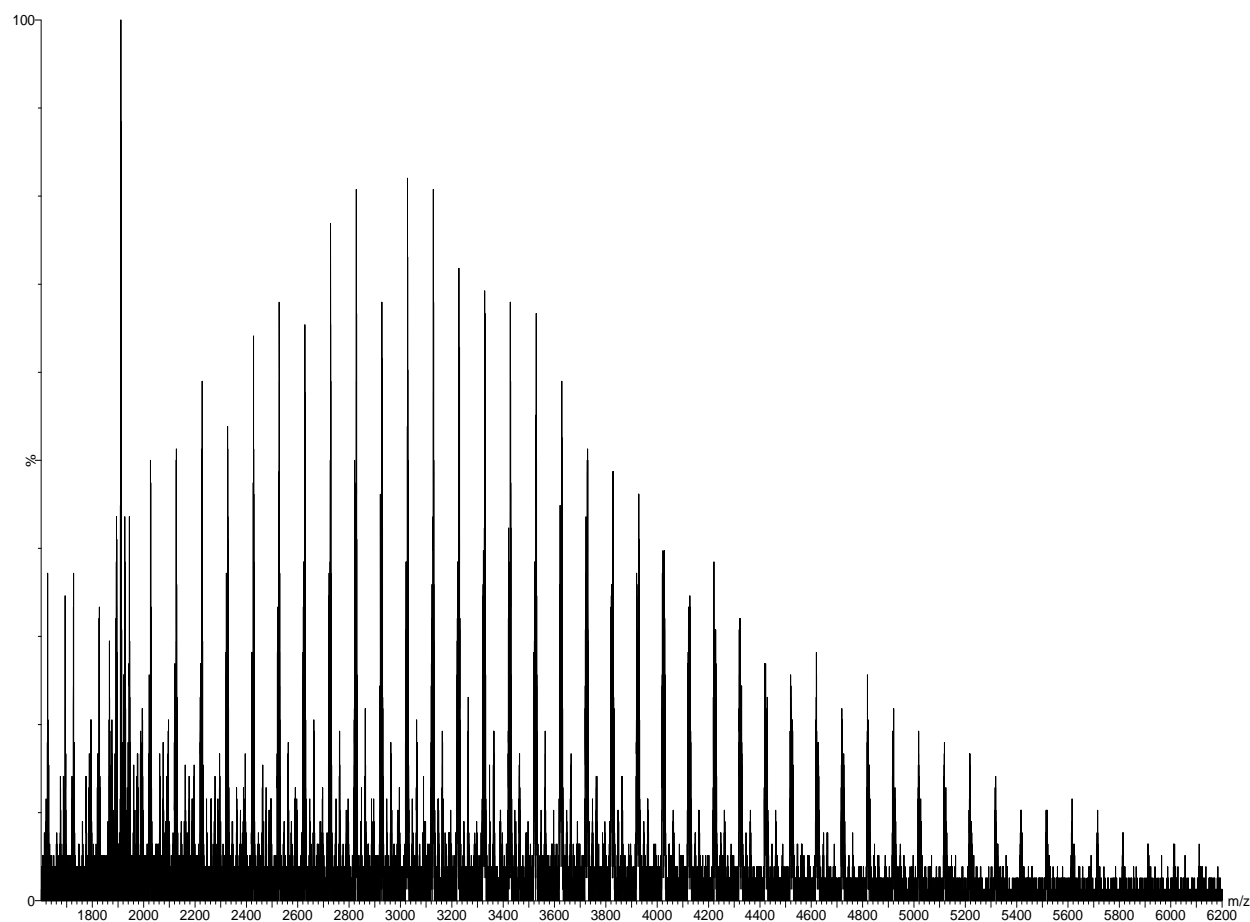| Parameter	Setting
Capillary Voltage	2900
Sample Cone Voltage	100
Extraction Cone Voltage	2.0
Source Temperature (°C)	90
Desolvation Temperature (°C)	150
Cone Gas Flow Rate (L/hr)	0
Desolvation Gas Flow Rate (L/hr)	500
Syringe Pump Flow Rate (µL/min)	10.0

Analysis Time – 5 minutes

APPENDIX E. Spectrum and Parameters of PMMA 4000 with Dihexadecyldimethylammonium

Bromide.

Parameter	Setting
Capillary Voltage	2900
Sample Cone Voltage	140
Extraction Cone Voltage	2.0
Source Temperature (°C)	90
Desolvation Temperature (°C)	100
Cone Gas Flow Rate (L/hr)	0
Desolvation Gas Flow Rate (L/hr)	500
Syringe Pump Flow Rate (µL/min)	10.0

Analysis Time – 5 minutes

Appendix F. Spectrum and Parameters of PMMA 4000 with Tetrahexadecylammonium Bromide.

Parameter	Setting
Capillary Voltage	2900
Sample Cone Voltage	100
Extraction Cone Voltage	2.0
Source Temperature (°C)	90
Desolvation Temperature (°C)	150
Cone Gas Flow Rate (L/hr)	0
Desolvation Gas Flow Rate (L/hr)	500
Syringe Pump Flow Rate (µL/min)	10.0

Analysis Time – 5 minutes